

**An improved Convolutional Neural Network Strategy for**  
**Verification of Handwritten Signature Images**



**Haider Ali**

**Registration No: 175-FET/MSEE/F22**

**Supervisor:**

**Dr. Zeeshan Aslam Khan**

**Co Supervisor:**

**Dr. Khizer Mehmood**

**Department of Electrical and Computer Engineering**  
**Faculty of Engineering and Technology International**  
**Islamic University Islamabad**

**2024**

## **DISSERTATION**

A dissertation submitted to the Department of Electrical Engineering, International Islamic University Islamabad as a partial fulfillment of the requirements for the award of the degree.

**Department of Electrical Engineering  
Faculty of Engineering and Technology  
International Islamic University Islamabad**

**2024**

## **DEDICATION**

This thesis is dedicated to my beloved parents, respected teachers and all those who prayed for my success in my life's endeavors.

“Alhamdulillah for everything, we can never thank Almighty Allah Pak enough for the countless bounties He blessed us with”

## **DECLARATION**

I certify that research work titled “An improved Convolutional Neural Network Strategy for Verification of Handwritten signature Images” is my own work and has not been presented elsewhere for assessment. Moreover, the material taken from other sources has also been acknowledged properly.

## **ACKNOWLEDGEMENT**

First of all, I am greatful to ALLAH (SWT), the Almighty, the creator of heavens and the earth, the most Merciful, the most Compassionate for blessing me with great parents, supportive teachers and co-operative friends. I couldn't have completed my Research-work without His guidance and blessings.

This work is completed with the help of two people, supervisor Dr. Zeshan Aslam Khan and co-supervisor Dr. Khizer. With out their continuous support, motivational strength, valuable guidance, sincere devotion, and most importantly their valuable time, Otherwise I would not have completed this research.

In the last, I am very thankful to my mom and dad for their continuous support, unconditional love. They have always given me the moral and spiritual support and motivation to achieve my goals.

## **ABSTRACT**

Biometric authentication systems have evolved significantly during recent times, with signature verification still used in conjunction with other modalities, including, fingerprint, facial recognition, and iris scan for identity verification purposes. The aim of signature verification is to determine whether the given signature is real or not, via comparison with reference signature stored in the database. Signature verification is categorized in to two types, online which involves verifying signatures in real-time, and offline which involves verifying signatures from static image. Offline signature verification is a challenging task, since real-time information about signing process is not available, and the most important drawback associated with them is intra-class variability. In the literature, various deep learning techniques have been employed. These architectures required a substantial time and computational resources due to their complex architectures. This study introduces a writer-independent offline system based on explainable lightweight convolutional neural network, which uses generalized fractional order based optimization strategy. The proposed approach leverages the strength of lightweight CNN architecture to reduce computational resources, and incorporates explainable framework to enhance transparency, as opposed to established models which lack in computational efficiency and interpretability. Moreover the suggested model outshines current state of the art (SOTA) architectures on benchmark CEDAR database with 98% classification accuracy, and is also evaluated in terms of F1-score, precision, and recall.

## List of Figures

Figure 1: General overview of Machine Learning vs Deep Learning.....	- 04 -
Figure 2: Block diagram of CNN .....	- 05 -
Figure 3: Graphical Workflow of the Proposed Study.....	- 16 -
Figure 4: Sample Images from Benchmark CEDAR database at random .....	- 17 -
Figure 5: Proposed Ultralight Architecture's Block diagram.....	- 20 -
Figure 6: Structural Depiction of Ultralight CNN architecture .....	- 21 -
Figure 7: Graphical Abstract of Lime .....	- 24 -
Figure 8: Acc and Loss Plots, along with Confusion Matrix for Ultralight CNN with SGD .....	- 29 -
Figure 9: Acc and Loss Plots, along with Confusion Matrix for Ultralight CNN with FA-SGD ( $\alpha = 0.1$ ) .....	- 30 -
Figure 10: Acc and Loss Plots, along with Confusion Matrix for Ultralight CNN with FA-SGD ( $\alpha = 0.2$ ).....	- 31 -
Figure 11: Acc and Loss Plots, along with Confusion Matrix for Ultralight CNN with FA-SGD ( $\alpha = 0.3$ ).....	- 32 -
Figure 12: Acc and Loss Plots, along with Confusion Matrix for Ultralight CNN with FA-SGD ( $\alpha = 0.4$ ) .....	- 33 -
Figure 13: Acc and Loss Plots, along with Confusion Matrix for Ultralight CNN with FA-SGD ( $\alpha = 0.5$ ).....	- 34 -

Figure 14: Acc and Loss Plots, along with Confusion Matrix for Ultralight CNN with FA-SGD ( $\alpha = 0.6$ ) .....	- 36 -
Figure 15: Acc and Loss Plots, along with Confusion Matrix for Ultralight CNN with FA-SGD ( $\alpha = 0.7$ ) .....	- 37 -
Figure 16: Acc and Loss Plots, along with Confusion Matrix for Ultralight CNN with FA-SGD ( $\alpha = 0.8$ ) .....	- 38 -
Figure 17: Acc and Loss Plots, along with Confusion Matrix for Ultralight CNN with FA-SGD ( $\alpha = 0.9$ ) .....	- 39 -
Figure 18: Acc and Loss Plots, along with Confusion Matrix for Ultralight CNN with FA-SGD ( $\alpha = 1.0$ ) .....	- 40 -
Figure 19: Acc and Loss Plots, along with Confusion Matrix for Ultralight CNN with FA-SGD ( $\alpha = 1.1$ ) .....	- 42 -
Figure 20: Acc and Loss Plots, along with Confusion Matrix for Ultralight CNN with FA-SGD ( $\alpha = 1.2$ ) .....	- 43 -
Figure 21: Acc and Loss Plots, along with Confusion Matrix for Ultralight CNN with FA-SGD ( $\alpha = 1.3$ ) .....	- 42 -
Figure 22: Acc and Loss Plots, along with Confusion Matrix for Ultralight CNN with FA-SGD ( $\alpha = 1.4$ ) .....	- 45 -
Figure 23: Acc and Loss Plots, along with Confusion Matrix for Ultralight CNN with FA-SGD ( $\alpha = 1.5$ ) .....	- 46 -

Figure 24: Acc and Loss Plots, along with Confusion Matrix for Ultralight CNN with FA-SGD ( $\alpha = 1.7$ ) .....	- 48 -
Figure 26: Acc and Loss Plots, along with Confusion Matrix for Ultralight CNN with FA-SGD ( $\alpha = 1.8$ ) .....	- 49 -
Figure 27: Acc and Loss Plots, along with Confusion Matrix for Ultralight CNN with FA-SGD ( $\alpha = 1.9$ ) .....	- 50 -
Figure 28: Combined Learning Curve visualization of training accuracy trends for Study-I .....	- 51 -
Figure 29: Combined Learning Curve visualization of validation accuracy trends for Study-I .....	- 54 -
Figure 30: Combined Learning Curve visualization of training loss trends for Study-I .....	- 54 -
Figure 31: Combined Learning Curve visualization of validation loss trends for Study-I .....	- 55 -
Figure 32: Combined Learning Curve visualization of training accuracy trends for Study-II .....	- 56 -
Figure 33: Combined Learning Curve visualization of validation accuracy trends for Study-II .....	- 56 -
Figure 34: Combined Learning Curve visualization of training loss trends for Study-II .....	- 57 -
Figure 35: Combined Learning Curve visualization of validation loss trends for Study-II .....	- 57 -

Figure 36: Combined Learning Curve visualization of training accuracy trends for Study-III .....	- 58 -
Figure 37: Combined Learning Curve visualization of validation accuracy trends for Study-III .....	- 58 -
Figure 38: Combined Learning Curve visualization of training loss trends for Study-III .....	- 59 -
Figure 39: Combined Learning Curve visualization of validation loss trends for Study-III .....	- 59 -
Figure 40: Combined Learning Curve visualization of training accuracy trends for Study-IV .....	- 60 -
Figure 41: Combined Learning Curve visualization of validation accuracy trends for Study-IV .....	- 60 -
Figure 42: Combined Learning Curve visualization of training loss trends for Study-IV .....	- 61 -
Figure 43: Combined Learning Curve visualization of validation loss trends for Study-IV .....	- 61 -
Figure 44: Interpretable Predictions by Ultralight CNN Architecture .....	- 62 -

## List of Tables

Table 1: Overview of CNN architectures .....	- 06 -
Table 2: Data Preprocessing steps.....	- 19 -
Table 3: Architecture Parameters of Ultralight CNN model.....	- 21 -
Table 4: Evaluation Metrics .....	- 25 -
Table 5: Performance analysis of Study-I (Precision (PC), Recall (RC), F1-Score (FS) on test set, along with Loss (LS) and Accuracy (AC) on train,validation and test sets .....	- 35 -
Table 6: Performance analysis of Study-II (Precision (PC), Recall (RC), F1-Score (FS) on test set, along with Loss (LS) and Accuracy (AC) on train,validation and test sets .....	- 35 -
Table 7: Performance analysis of Study-III (Precision (PC), Recall (RC), F1-Score (FS) on test set, along with Loss (LS) and Accuracy (AC) on train,validation and test sets .....	- 47 -
Table 8: Performance analysis of Study-IV (Precision (PC), Recall (RC), F1-Score (FS) on test set, along with Loss (LS) and Accuracy (AC) on train,validation and test sets .....	- 47 -
Table 9: Comparative Analysis with existing benchmark models on CEDAR dataset .....	- 53 -

# Table of Contents

<u>CHAPTER 1</u> .....	- 1 -
<u>INTRODUCTION</u> .....	- 1 -
<u>1.1</u> <u>Introduction</u> .....	- 1 -
<u>1.2</u> <u>Inspiration and Background</u> .....	- 1 -
<u>1.3</u> <u>Problem Statement</u> .....	- 7 -
<u>1.4</u> <u>Goals and Objectives</u> .....	- 9 -
<u>1.5</u> <u>Thesis Organization</u> .....	- 9 -
<u>CHAPTER 2</u> .....	- 11 -
<u>LITERATURE REVIEW</u> .....	- 11 -
<u>2.1</u> <u>Introduction</u> .....	- 11 -
<u>2.2</u> <u>Previous work</u> .....	- 11 -
<u>2.3</u> <u>Our Work</u> .....	- 14 -
<u>2.4</u> <u>Summary</u> .....	- 14 -
<u>PROPOSED METHODOLOGY</u> .....	- 15 -
<u>3.1</u> Introduction .....	- 15 -
<u>3.2</u> Dataset Description.....	- 15 -
<u>3.3</u> Data Preprocessing.....	- 16 -
<u>3.4</u> Ultralight CNN .....	- 17 -
<u>3.5</u> Evaluation Metrics .....	- 19 -
<u>3.6</u> Local Interpretable Model-Agnostics Explanation (LIME) .....	- 19 -
<u>3.7</u> Fractionally Accelerated Stochastic Gradient Descent (FA-SGD) .....	- 22 -
<u>3.8</u> Summary .....	- 25 -
<u>CHAPTER 4</u> .....	- 27 -
<u>SIMULATIONS AND ANALYSES</u> .....	- 27 -
<u>4.1</u> <u>Introduction</u> .....	- 27 -
<u>4.2</u> <u>Study-I</u> .....	- 27 -
<u>4.3</u> <u>Study-II</u> .....	- 28 -

<u>4.4</u>	<u>Study-III</u>	.....	- 41 -
<u>4.5</u>	<u>Study-IV</u>	.....	- 41 -
<u>4.6</u>	Discussion	.....	- 52 -
<u>4.7</u>	<u>Comparison with existing Benchmark Models</u>	.....	- 52 -
<u>4.8</u>	Predictive Strength	.....	- 53 -
<u>4.9</u>	Summary	.....	- 62 -
	<u>CHAPTER 5</u>	.....	- 63 -
	<u>CONCLUSIONS AND FUTURE WORK</u>	.....	- 63 -
<u>5.1.</u>	<u>Introduction</u>	.....	- 64 -
<u>5.2</u>	<u>Conclusions</u>	.....	- 63 -
<u>5.2</u>	<u>Future Work</u>	.....	- 64 -
	<u>REFERENCES</u>	.....	- 65 -

# CHAPTER 1

## INTRODUCTION

### 1.1 Introduction

This chapter deeply elaborates the need, importance, and valuable applications of biometrics and its modes. It also describes signature verification along with its modes, as well as the advantages associated with it, such as its versatility and ease of implementation. This chapter further discusses solutions to signature verification, which include various artificial intelligence techniques. This chapter also discusses various challenges associated with signature verification task and emphasizes on deep learning for signature verification tasks, especially the convolutional neural networks which offers better accuracy in contrast to traditional machine learning approaches. This chapter also necessitates the development of lightweight convolutional neural network model in order to cater to computational complexity and reduce resource intensive requirements and training time. Finally, an introduction of the proposed light weight convolutional neural network for signature verification task is presented.

### 1.2 Inspiration and Background

Biometrics deals in automatically recognizing individuals based on physical or behavioral traits, such as facial features, fingerprints, iris patterns, hand, voice, gait, and signatures to automatically recognize and identify individuals [1]. Biometrics finds tremendous applications in various fields and industries, including Identity Verification [2], Time and Attendance Tracking [3], Forensic Identification [4], Healthcare [5], Financial Services [6], Government Services [7], Education [8] and Customer Services [9], etc. One mode of biometric authentication is via signature verification, which involves analyzing and comparing the unique characteristics of individual's handwritten signatures to authenticate their identity.

Signature Verification process determines, whether the given signature matches known or reference signature for particular individual. It is used for authentication and fraud detection ensuring that the signature is genuine and made by authorized person. Signature verification typically involves comparing various features, e.g., stroke patterns, shape, size, pressure, and timing, with a reference signature stored in a database. There are two modes associated with verification of signatures, “offline” and “online”. Offline verification mode involves analyzing a static image, without any real-time interaction with the signer i.e., captured on physical documents, such as paper forms, contracts, or checks, while online mode involves capturing the signature dynamically as it is being written, often using specialized hardware such as digitizing tablets or touchscreens. This mode allows for the analysis of additional features such as pen pressure, velocity, and acceleration, providing more detailed information for authentication.

The main advantages of signature verification over other biometrics are its versatility and ease of implementation in various scenarios. Signature verification does not require direct contact with a sensor or device, unlike fingerprints or iris scans. This non-intrusive nature makes it more user-friendly, both offline and online signature verification can be seamlessly integrated into existing document-based workflows, such as signing contracts, authorizing transactions, or verifying identity. This convenience makes it ideal for various applications, from banking to legal documentation. Implementing signature verification systems, particularly offline methods, can be relatively low-cost compared to biometric systems that require specialized hardware like fingerprint scanners or iris readers. Offline signature verification relies on digital scanners or cameras, which are often more affordable and widely available. Signature verification systems can adapt to different use cases and scenarios. Offline signature verification, for example, allows individuals to verify signatures on paper documents, while online verification enables real-time authentication in digital environments such as e-commerce platforms or online forms. Overall, the flexibility, convenience, and cost-effectiveness of signature verification, in both

offline and online modes, make it a preferred choice for many applications, offering advantages over other biometric modalities in certain scenarios.

Solutions for the recognition and verification of signatures can be classified as, Machine Learning (ML) techniques, that rely on manually crafted feature extraction mechanisms [10], and deep learning methods [11, 12] that involve neural networks such as Convolutional Neural Networks (CNNs) [13, 14] or Recurrent Neural Networks (RNNs) [15, 16], to learn hierarchical representations of signatures directly from raw pixels. These models automatically gather discriminative features from signatures, and can potentially achieve higher accuracy compared to traditional handcrafted feature-based methods [10]. Deep learning (DL) methods are regarded as very promising due to their mindblowing capability in image recognition and detection [17]. Hand-crafted techniques for the extraction of features include, Discrete cosine transform (DCT), Local Features (Speeded-Up Robust Features (SURF), Scale-Invariant Feature Transform (SIFT), Local Binary Patterns (LBP), etc.) [18, 19], Global Features (Shape Matrices, Invariant Moments etc.) [20], Gaussian Mixture Model (GMM) [21], Curvelet transform [22], Contourlet Transform (CT) [23], and Gabor wavelet [24], etc. While DL techniques involve neural networks to extract features, autonomously discovering useful representations or features within the data without the need for manual annotation or supervision [12, 25].

DL is branch of ML that focuses on neural networks and their ability to learn and make decisions that replicate the brain of human being, which consists of neurons, each receiving an input signal, processing it, and producing an output signal and than transmitting it to next one. Similarly in neural networks, artificial neurons (nodes) which are termed as perceptron receive inputs, apply an activation function, and produce an output signal which is moved on to the subsequent layers. **Fig-1** provides a general overview of machine learning and deeplearning, indicating handcrafted feature extraction mechanisms in machine learning while the deep learning approach automatically extract features via

deep neural network.

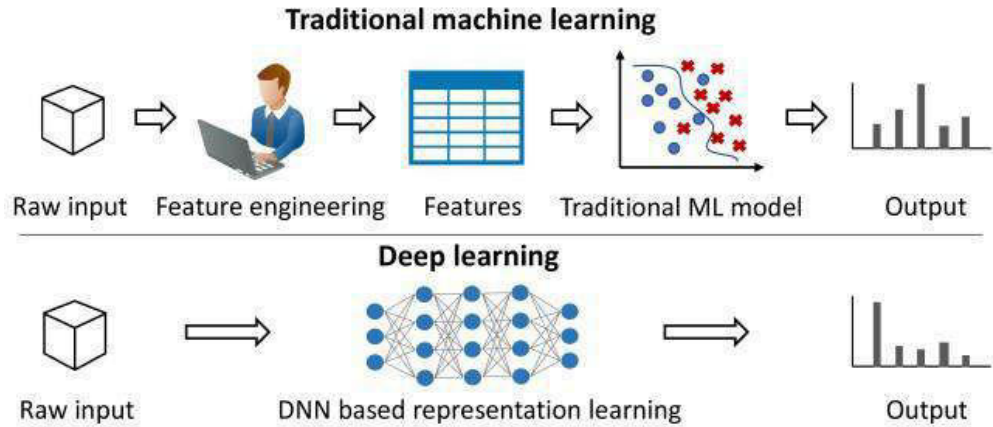


**Fig-1: General overview of Machine Learning vs Deep learning**

Now a days DL has surfaced as pivotal tool in pattern recognition, Natural Language Processing (NLP), and Computer vision, etc. One of the deep learning approach is CNNs, which are tailored for processing data in structured patterns e.g., images and videos. CNNs comprise of series of convolutional, pooling, and fully connected (FC) layers, responsible for extraction of useful features, reduction in dimentionality, and classification purposes, Where FC layers receives feature maps as a one-dimensional flattened array. Block diagram of simple CNN architecture comprising of two layers is presented in **Fig-2**.

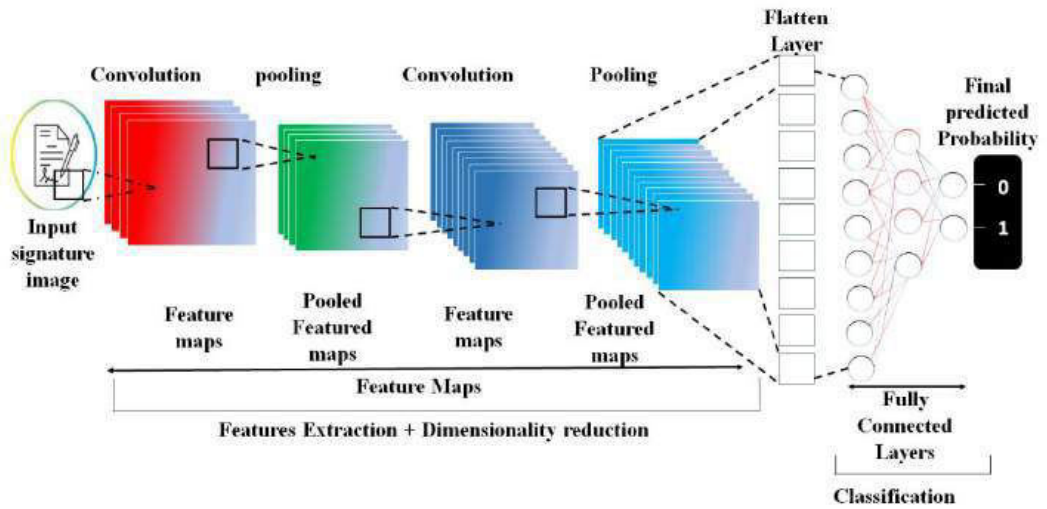


**Fig-2: Block diagram of CNN**

Convolutional Neural Networks (CNNs) were first introduced in the late 1980s. In 1998, Yann LeCun, along with his collaborators, proposed the pioneering LeNet-5 architecture, which was one of the earliest implementations of CNNs, achieving SOTA performance on MNIST database, a dataset comprising of handwritten digits. LeNet-5 architecture comprised of three convolutional layers with filter size of 5x5, two average pool and two FC layers, with final FC layer comprising of 10 neurons, representing digit classes from 0 to 9. CNN architecture have undergone various modifications from 1989 until today, which include structural reformulation, regularization, parameter optimizations, etc. LeNet-5 and subsequent developments in CNNs significantly contributed in advancing the realm of pattern recognition. Since then, CNNs have evolved significantly, with refinements in architectural designs, training techniques, and applications across diverse fields.

Up to date, several CNN architectures have been introduced, each having unique design characteristics and achieving SOTA performance on various image processing tasks. These architectures have significantly advanced the field of artificial intelligence and have been instrumental in solving challenging problems in image recognition, object detection, segmentation, and more. Some

of the notable CNN architectures include AlexNet, ResNet, Visual Geometry Group (VGG), Inception and High-resolution Network (HRNet) [26-31], etc.

**Table-1** illustrates some of the CNN architectures, taking in to consideration the number of convolutional layers, pooling layers, strides, kernel size, and activation functions utilized in these architectures starting from AlexNet to much deeper networks such as Inception-ResNet-v2 and ResNext-50.

**Table-1: Overview of CNN architectures**

Model	Year	Variants	Architecture	kernel size	Strides	Activation Function
<b>AlexNet</b>	2012	-----	Convolutional layers: 5, Pooling layers: 3, Fully Connected layers: 3	11x11 5x5 3x3	4	Relu, Softmax
<b>VGG</b>	2013	VGG-16 VGG-19	Convolutional layers:13,16 Pooling:5 Fully Connected: 3	3x3	1	Relu, Softmax
<b>ResNet</b>	2015	ResNet-18, 34, 50,101, 110,152,164	Convolutional layers:17 up to 166 in ResNet-164 Pooling layers: 2 Fully connected: 1	7x7 1x1 3x3	2	Relu, Softmax
<b>Inception</b>	2014	Inception-v1, v2, v3,v4, Inception-ResNet-v2	59 convolutional layers (57 in stem and inception modules), 15 pooling, 6 fully connected layers in inception-v1 up to 244 convolutional layers in Inception-ResNet-v2	1x1 3x3 5x5 1x7 7x1 1x3 3x1	2,1	Relu, Softmax
<b>ResNeXT-50</b>	2017	-----	Convolutional layers: 53 Pooling layers: 2 Fully Connected: 1	1x1 3x3 7x7	2	Relu,Softmax

A lot of work has been done on Signature verification, Signature verification just

like other biometric verification is performed by various means, traditional machine learning approaches which include preprocessing, handcrafted feature extraction techniques for feature extraction, feature learning and then classification via support vector machines or K Nearest neighbour (KNN) to characterize signature as genuine or forged, Fully connected feed forward neural network (FCFNNs) also known as Artificial Neural Network can also be utilized for feature extraction along with it KNN or SVMs for classification. CNNs which are specially designed to handle grid like structures, have become very popular in image and video processing, can also be utilized , and have demonstrated SOTA performance in signature verification, outperforming ML and other deep learning methods. Transfer Learning approaches utilizing pre-trained models, such as VGG-16, Inception, ResNet, etc. which were initially trained on large image datasets, are fine-tuned by applying certain modifications are also utilized for signature verification tasks. RNNs designed to handle time-series or ordered data, have also been explored recently for signature verification, but their performance is not up to the mark as compared to CNNs. Hybrid approaches utilizing the strength of CNNs and RNNs have also shown promising results. The choice among all these methods hinges upon specific application requirements, available resources, and the desired level of accuracy.

### 1.3 Problem Statement

Verification of handwritten signatures is difficult task to accomplish due to human hand writing which varies over time hence individuals may exhibit differences in signatures resulting in complications to establish single reference model. Forgeries or imitations by anyone trying to trick the verification mechanism are possible with signatures, furthermore signature verification system requires large no of genuine samples for training to ensure good generalization on data which is never seen before by model. Since the access to genuine signatures is limited due to privacy concerns while forgeries are common hence leading to imbalances in data. Complexities can also be introduced by low-quality or low-resolution samples, thus introducing noise that

leads the model to learn from noisy gradients, resulting in reduced accuracy and an increased error rate. To tackle these problems successfully, SOTA artificial intelligence (AI) based algorithms must frequently be developed, in addition to this large and varied datasets containing signatures of varied languages, background and hand writing styles should be gathered for training purposes. Moreover, to enhance robustness of systems devoted to handwritten signature verification, techniques such as data augmentation must be employed to handle variability to input data. The computational complexity associated with existing models is also one of the key problems, since most of CNN models are resource-intensive, require substantial training time and computational resources, this necessitates the development of lightweight CNN model, having simple architecture and less parameter count.

This study proposes an ultralight CNN for verification of handwritten signatures, having a customized feature extraction mechanism, incorporating several convolutional, pooling and normalization layers. An interpretable artificial intelligence (XAI)-based local interpretable model-agnostics explanation (LIME) technique is also utilized to offer insights into the predictions by the suggested model. Data augmentation is exploited in order to enhance the suggested model's ability to generalize effectively for varied signature samples. The architectures studied previously remain quite laudable, but are very complex and resource intensive as opposed to the proposed strategy which seems to be resource friendly. In addition to this, the fractional calculus based optimization strategy is adopted, i.e. the fractional stochastic gradient descent (FSGD) which has shown promising results in recommender systems disciplines [32-34], speeding up the convergence of SGD by adaptively adjusting the learning rate. Recently introduced generalized version of FSGD, i.e., GFSGD [35] is also implemented to solve recommender system problem [36], which provides greater fractional order range in comparison to FSGD, where it lies between 0 and 1.

## 1.4 Goals and Objectives

- To accurately differentiate between signatures and forgeries for secure and reliable identity verification.
- To employ a customized ultralight CNN variant specifically designed for signature verification, delivering a thorough analysis through its capacity for autonomous feature extraction and learning.
- To explore the impact of fractional calculus in enhancing the robustness and accuracy of signature verification.
- To accelerate the speed of convergence by exploiting novel FA-SGD optimization algorithm for verification of signatures.
- To investigate LIME approach for generating interpretable predictions by suggested ultralight CNN, offering transparency and reliability in signature verification domain.

## 1.5 Thesis Organization

**Chapter 1:** provides a conceptual overview of the entire thesis, consisting of research gaps, statements, and definitions that clearly define research goals and hypotheses, as well as background and motivations for the determination of problematic issues and research problem definitions.

**Chapter 2:** provides detail of the work done so far by discussing the advantages and disadvantages of already suggested methods in literature.

**Chapter 3:** describes the methodology of conducted research by elaborating the suggested ultralight model along with FA-SGD optimization strategy. It also contains the pseudocode of the proposed model.

**Chapter 4:** provides simulation results in terms of tables and learning curves for a detailed comparison of the suggested ultralight CNN with the standard SGD and the novel FA-SGD optimization algorithm using benchmark CEDAR dataset.

**Chapter 5:** holds the conclusions deduced from the conducted research work, also includes future initiatives which can be taken for the extension of conducted research..

# Chapter 2

## LITERATURE REVIEW

### 2.1 Introduction

This chapter includes AI models deployed by various authors for task of signature verification on benchmark datasets. Some of the previous work regarding signature verification is described below. Additionally, this chapter also includes our contributions and a summary at the end.

### 2.2 Previous Work

In recent years, significant strides have been made in developing classifiers for signature recognition and verification, using various machine learning and deep learning algorithms. Deep learning approach has emerged powerful, and has demonstrated notable improvement for signature verification tasks in terms of accuracy on various datasets. Some of the previous work has been described below.

Stauffer, M., et al. [37] integrated both the local and global changes utilizing Dynamic Time Warping, previous methods regarding this employ global matchings where the entire graph structures representing handwritten entities were compared directly. Sharif, M., et al. [38] proposed an offline signature verification system utilizing Genetic algorithm for feature selection from extracted set of features and Support Vector Machines for classification. Radhika, K.S., and Gopika, S. [39] both modes to form an integrated approach. In order to explore the applications of shape and size based features, i.e. geometric, Chandra, S., and Maheskar, S. [40] proposed an offline verification system based on Artificial Neural Network.

Verification system based on 15 global features and remaining extracted from freeman chain Code is presented in [41], while utilizing k-nearest neighbour for classification and was tested on MCYT dataset. Dey, Sharma, N., et al. [42]

presented a framework known as Siamese Network consisting of identical subnetworks which work by minimizing and maximizing Euclidean distance between similar and dissimilar pairs. Since forgeries are not available in real world scenarios to train the model, Shariatmadari, S., et al. [43] suggested deep learning based approach which aimed at capturing local variations with in signatures and model was trained on single class, i.e. genuine. Wei, P., Li, H., and Hu, P. [44] introduced an inverse discriminative network employing four weight-shared streams to extract features. Recent advancements in signature verification include work such as recurrent neural networks [16] based approach, graph neural network [45] utilizing graph structures to learn representations, combining CNNs with Capsule Networks [46] and encoder-decoder architecture for self-supervised learning, i.e.“SURDS” [47].

Sanmorino, A., and Yazid, S. [48] advocated for Artificial Neural Networks and hidden Markov models (HMM) for verification, considering factors like data availability and budget. To enhance feature extraction stage in offline verification Alsuhimat, F., and Mohamad, F. S. [49] proposed hybrid method combining features from CNN and HOG and used Long Short-Term Memory (LSTM), K Nearest Neighbour (KNN), and SVM as classifiers. Hybrid architectures [50] combining CNN and RNN, utilizing strength of CNN for extraction of features, and RNNs for gathering long range dependencies from signature image have also been popular these days. Researchers have also worked on feature fusion, integrating features from both writer independent and writer dependent classifiers earlier work done regarding this was hybrid WI-WD [51] scheme, later work included further investigation of robustness on GPDS signature database [52].

Signature verification system requires significant amount of training samples, contradicting this notion Kao, H.-H., and Wen, C.-Y. [53] indicated that accuracy up to 99.96% can be obtained by utilizing single genuine signature for training through local features. Hirunyawananakul, A., et al. [54] compared accuracies from transfer learning using pretrained VGG-16, and AlexNET with

CNN developed from scratch and traditional ML approach, transfer learning approach outperformed others with 100% accuracy. Mitchell, A., et al. [55] obtained accuracy of 86.7% using pre-trained VGG-16 on balanced dataset that underwent through data augmentation. Mersa, O., et al. [56] obtained EER of 3.98% on MCYT-75 utilizing pretrained weights of ResNet-8. Jampour, M., et al. [57] integrated the regularized Capsule Networks (CapsNet) with ResNet, utilizing feature extraction strength of ResNet, and positional understanding capabilities of CapsNet, the integrated approach lead to accuracy of 99.85% on CEDAR and 99.24% on MCYT.

In 2019 Jahandad, S., et al. [58] used pretrained models, Inception-v1 and Inception-v3 for signature verification on GPDS Synthetic, and achieved 83% validation accuracy using samples from 20 users via Inception-v1 as opposed to 75% through Inception-v3, which indicated overfitting of ultradeep 42 layered Inception-v3. In 2019 Gumusbas, D., and Yildirim, T. [59] demonstrated that Capsule Network significantly outperform CNN-based model for offline signature verification, achieving higher accuracy with minimal data, and maintaining effective feature extraction even at lower resolution. In 2023 Muhtar, Y., et al. [60] reduced computational cost and parameter size of ResNet-18 by fusing it with convolutional block attention modules with this approach accuracy was increased to 96% from initial 95% on CEDAR dataset. In 2023 Tanko, O., et al. [61] achieved accuracy of 91.3% and absolute error rate of 7.45% on CEDAR the proposed method utilized VGG-16 for feature extraction along with it SVM was used as classifier.

Researchers have made significant strides to speed up CNNs, that is divided into three categories which include, optimization implementation [62], which enables learning in few iterations, binarization and parameter quantization [63] and architectural simplification [64] . He, Y., et al. [65] introduced new channel pruning technique to quicken deep CNNs, the proposed approach speeded up VGG-16 five times with only 0.3% increment in error. Taking into consideration the structural simplicity a cutting-edge ultralight convolutional neural network

for efficient verification of handwritten signatures is presented in this study, along with it a novel fractionally accelerated stochastic gradient decent (FA-SGD) optimization strategy is employed, inspired by its effectiveness in solving recommender systems task [36], has prompted us to investigate its capabilities in image classification, specifically in signature verification. The suggested ultralight CNN with novel FA-SGD optimization approach has shown significant performance as compared to the SOTA models by using simple architecture, innovative pooling strategy and unexplored optimizer.

### 2.3 Our Work

The task of signature verification for authentication brings us to a model, which verifies the signature in two classes i.e., genuine or forged. The summary of our contributions are:

- A novel Ultralight CNN architecture is proposed, with a less number of layers hence less computational cost.
- Robust CNN model, incorporating data augmentation and customized feature extraction mechanism via Channel split dual attention and mixed pooling.
- To enhance the speed of convergence to achieve optimal parameters by exploiting novel FA-SGD optimizer for classification of signature images.
- LIME is exploited to provide explainable predictions.
- The ultralight CNN outperforms already present SOTA models in various evaluation metrics on benchmark CEDAR database.

### 2.4 Summary

This chapter has provided detailed overview of Literature on signature verification. The next chapter provides the methodology of conducted research

# Chapter 3

## Proposed Methodology

### 3.1 Introduction

This chapter provides a comprehensive overview of the suggested ultralight CNN model for verification of handwritten signatures, based on generalized fractional optimization. The methodology consists of several stages, including:

- Dataset description
- Data preprocessing
- Lightweight CNN model development
- Evaluation metrics selection
- LIME
- FA-SGD

### 3.2 Dataset description

CEDAR database comprise of offline signatures, having signatures from 55 distinct signers, with each individual contributing 24 authentic samples, and 24 meticulously crafted forgeries. Therefore accommodating 2640 signature samples. Each signature in CEDAR database is scanned at 300 dpi resolution, than converted to binary image using a grayscale histogram. Every signature was produced by using black pen. In this study we have splitted dataset in to train, validation, and test sets. Seventy percent of samples are allocated to training set, and remaining thirty percent are split equally (15% each) for the validation and test sets. **Fig-4**, presents some samples from CEDAR database utilized in the study.

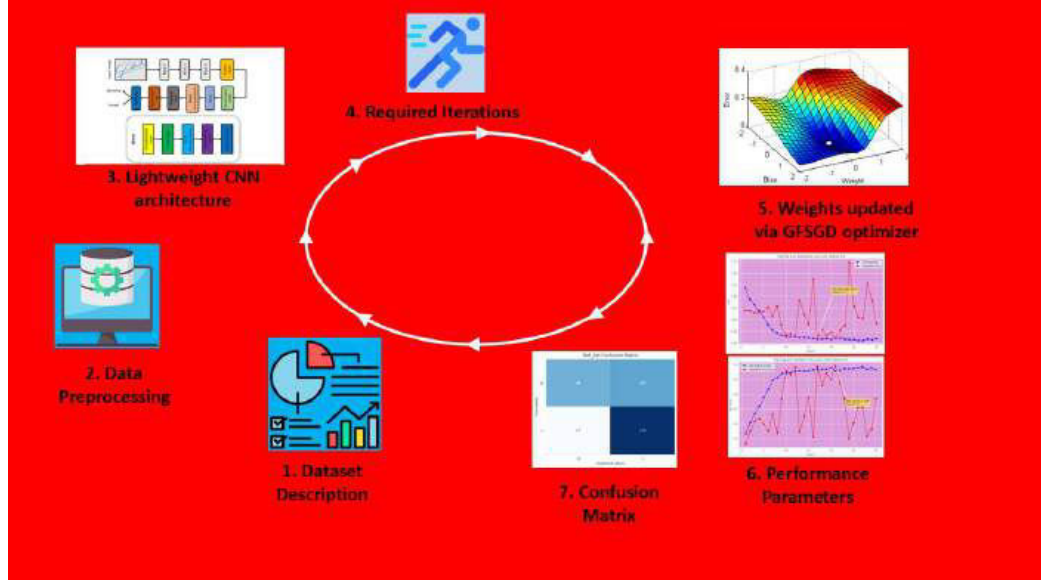


**Fig-3: Graphical Workflow of the Proposed Study**

### 3.3 Data Preprocessing

Preprocessing is a crucial phase [66] in preparing raw data to be effectively used by machine learning algorithms. To ensure the effectiveness of machine learning strategy, data preprocessing needs to be done adequately for learning latent features from signature images. To make our study robust and adaptable, several pre-processing steps are exploited on the benchmark CEDAR database for reducing variability in image quality and size, enhancing discriminative power of signature images, and improving generalization ability of deep learning model. These preprocessing steps include:

- Splitting database into train set, validation set, and test set.
- Creating data generators for efficient loading, and augmentation of images.
- Resizing images to a fixed size of (224, 224) pixels.
- Normalizing or transforming pixel values to fall in range [0, 1].
- Converting class labels to categorical values.
- Performing data augmentation on the training set, including horizontal

flipping of images.

**Table-2**, shows the data pre-processing steps exploited in the study.



**Fig-4: Sample Images from benchmark CEDAR database at random**

### 3.4 Ultralight CNN

CNN has been exploited in computer vision related problems because of its exceptional capabilities in dimensionality reduction, and feature extraction, enabling effective image analysis and processing. Given their exceptional performance in feature extraction and dimensionality reduction, CNNs have emerged as a pillar in computer vision, driving breakthroughs in image classification, segmentation and various other image analysis tasks. This study suggests an ultralight CNN for handwritten signature's verification. Architectural depiction of suggested architecture is presented in **Fig-5**. The architecture comprise of four blocks, first three comprise of three convolutional layers, having custom built dynamic separable convolution with default filter size of 3x3 for depthwise convolution, with 16 filters in first block and 32 in second and third blocks. Depthwise convolution is followed by pointwise convolution which performs channel-wise convolution and generate final output. All first three blocks comprise of relu activation function to introduce non-linearity, batch normalization to normalize the outputs of activation function, max pooling layer that downamples the output of batch normalization having a pool size of 3x3 and strides of 2x2 and a drop out layer that randomly drops 20% of output units to prevent overfitting. Custom

built channel split dual attention is also incorporated in third block which comprise of two convolutional layers, i.e. avg and max. Avg layer generates attention weights that focuses on the average features, while max layer generates attention weights that focuses on the most important features. The output of both is fed in to sigmoid activation function for normalization of attention weights. The input tensor is then element-wise multiplied with attention weights to generate weighted inputs. The weighted inputs are concatenated along the channel axis, combining both attention stream outputs. Fourth block comprises a flatten layer, followed by two FC layers with 128 and 64 units respectively, using ReLU activation and dropout with a rate of 0.2. Last one is output layer, i.e., Softmax with two units, representing the two signature classes. The last block comprise of a flatten layer followed by two FC layers, where first FC has 128 units along with batch normalization, dropout and a relu, and second FC is the output layer, consisting of 2 units corresponding to no of classes in the classification task, which in our case are genuine class and forged class, having SoftMax as activation operator to produce class probabilities. The class with the highest probability output by the softmax function will be considered as predicted class. The structural representation of ultralight CNN model is presented in **Fig-6** and the detailed overview of parameters accommodated by proposed model for signature classification on benchmark CEDAR dataset is tabulated in **Table-3**

<b>Table-2: Data Preprocessing steps</b>	
<b>Input:</b> Database with full_org and full_forg directories.	
	<ul style="list-style-type: none"> <li>• The dataset is loaded from the "/content/signatures" directory.</li> <li>• Check class distribution for forged and genuine signature images.</li> <li>• Check for null-values residing in dataset.</li> <li>• Dataset is split into train, validation, and test with ratio of 7:1.5:1.5 by using train_test_split function from Scikit-learn.</li> <li>• Data generators are created for all three using the ImageDataGenerator from Keras. The generators are used to load and preprocess the images in batches.</li> <li>• Data augmentation is applied using ImageDataGenerator on train, test and validation sets. The augmentation includes horizontal flipping of images.</li> <li>• Following parameters are specified for train, validation and testing sets through ImageDataGenerator: <ul style="list-style-type: none"> <li>➢ Color Space: 'rgb'</li> <li>➢ Class Mode: 'Categorical'</li> <li>➢ Shuffle: 'True'(train, validation), 'False'(test)</li> <li>➢ Image Shape: (224,224)</li> <li>➢ Batch Size: 16</li> </ul> </li> <li>• Generated data generators to provide preprocessed images to model in batches</li> </ul>

### 3.5 Evaluation Metrics

The suggested ultralight model's performance is accessed via multiple evaluation metrics, i.e. Recall, Precision, F1-score and Accuracy enumerated in **Table-4**. Where trpos refers to true positives which are correctly predicted positive instances and trneg refers to correctly predicted negative instances, i.e. true negatives, where as flpos and flneg represent false positives and false negatives, respectively. Which are incorrectly predicted positive and negative instances respectively.

### 3.6 Local Interpretable Model-Agnostics Explanation (LIME)

ML models are regarded as black boxes [67-69] by the researchers, due to their decision making processes being difficult to understand and interpret, hence lacking transparency and explainability. Therefore, the deployment of explainable artificial intelligence (XAI) [67] is essential in order to explain their

inner workings to provide understanding of model's output. Regarding this a powerful technique, i.e. LIME is used, which explains the predictions made by machine learning models in a transparent and interpretable way . It is an explainable artificial intelligence (XAI) [67] technique which explains the behaviour of a ML model for a specific instance and does not employ any back-propagation or model specific steps, making it a model-agnostic approach [70, 71]. **Fig-7** illustrates visual representation of LIME workflow. LIME technique interprets the decision making process of AI models, and effectively bridges the gap between complex neural network architectures and explainability by explaining the predictions of complex models by utilizing a local surrogate model [72]

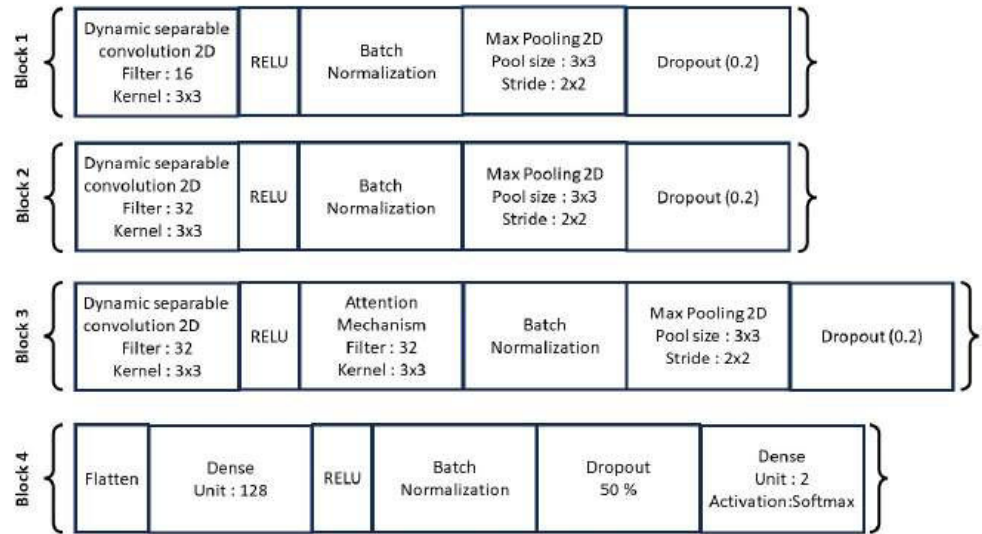


**Fig-5: Proposed Ultralight Architecture's Block diagram**

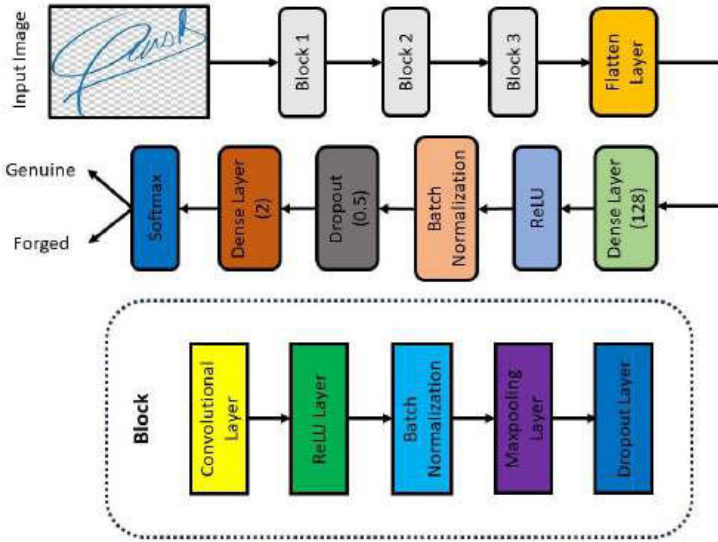


Fig-6: Structural Depiction of Ultralight CNN Architecture

Table.3: Architecture Parameters of Ultralight CNN model

Layer (type)	Output-Shape	Parameters
<b>Separable Dynamic Conv-2D</b>	(None,222,222,16)	<b>91</b>
<b>Activation</b>	(None,222,222,16)	<b>0</b>
<b>Batch-Norm</b>	(None,222,222,16)	<b>64</b>
<b>Max-Pooling2D</b>	(None,110,110,16)	<b>0</b>
<b>Drop-out</b>	(None,110,110,16)	<b>0</b>
<b>Separable Dynamic Conv-2D-1</b>	(None,108,108,32)	<b>688</b>
<b>Activation-1</b>	(None,108,108,32)	<b>0</b>
<b>Batch-Norm-1</b>	(None,108,108,32)	<b>128</b>
<b>Max-Pooling2D-1</b>	(None,53,53,32)	<b>0</b>
<b>Drop-out-1</b>	(None,53,53,32)	<b>0</b>
<b>Separable Dynamic Conv-2D-2</b>	(None,51,51,32)	<b>1344</b>
<b>Activation-2</b>	(None,51,51,32)	<b>0</b>
<b>Channel Split Dual Attention</b>	(None,51,51,64)	<b>18496</b>
<b>Batch-Norm-2</b>	(None,51,51,64)	<b>256</b>
<b>Max-Pooling2D-2</b>	(None,25,25,64)	<b>0</b>
<b>Drop-out-2</b>	(None,25,25,64)	<b>0</b>
<b>Flatten</b>	(None,40000)	<b>0</b>
<b>Dense</b>	(None,128)	<b>5120128</b>
<b>Activation-3</b>	(None,128)	<b>0</b>
<b>Batch-Norm-3</b>	(None,128)	<b>512</b>
<b>Drop-out-3</b>	(None,128)	<b>0</b>

Dense-1	(None,2)	258
<b>Total-params: 5141965 (19.62 MB)</b>		
<b>Trainable-params: 5141485 (19.61 MB)</b>		
<b>Non-trainable-params: 480 (1.88 KB)</b>		

### 3.7 Fractionally Accelerated Stochastic Gradient Descent (FA-SGD)

In SGD optimization approach, the parameters of model are updated iteratively to minimize loss function  $L(\theta)$ . The update rule is:

$$\theta_{t+1} = \theta_t - \eta \nabla_{\theta} L(\theta_t) \quad (1)$$

Where  $\theta_t$  and  $\theta_{t+1}$  are the model parameters at epoch t and t+1,  $\eta$  is the learning rate and  $\nabla_{\theta} L(\theta_t)$  is the gradient of loss w.r.t.  $\theta$  at iteration t.

FA-SGD introduces fractional calculus, where the conventional integer-order derivative is replaced with a fractional [35, 73, 74]. The Caputo fractional derivative of order  $\alpha$  for a function  $f(t)$  is defined as:

$${}^c D^{\alpha} f(t) = \frac{1}{\Gamma(n-\alpha)} \int_0^t \frac{f(n)(\tau)}{(t-\tau)^{\alpha-n+1}} d\tau \quad (2)$$

Where  $n-1 < \alpha < n$  and  $f(n)(\tau)$  is the  $n$ th derivative of  $f(\tau)$ . For  $0 < \alpha < 1$ , we use  $n=1$  and  $\Gamma(n-\alpha)$  is the Gamma function evaluated at  $n-\alpha$

$$\Rightarrow {}^c D^{\alpha} f(t) = \frac{1}{\Gamma(1-\alpha)} \int_0^t \frac{f'(\tau)}{(t-\tau)^{\alpha}} d\tau \quad (3)$$

Gradient descent algorithm is modified using Caputo fractional derivative, where  $L(\theta)$  is the loss function which is to be minimized, and  $\theta$  represents model parameters. The fractional gradient of  $L(\theta)$  with respect to  $\theta$  is given by:

$$\nabla_{\theta}^{\alpha} L(\theta) = \frac{1}{\Gamma(1-\alpha)} \int_0^{\theta} \frac{\partial L(\tau)}{\partial \tau} (0-\tau)^{-\alpha} d\tau \quad (4)$$

Using the Caputo fractional derivative, standard gradient  $\nabla_{\theta} L(\theta_t)$  is replaced by

fractional gradient  $\nabla_{\theta}^{\alpha}L(\theta_t)$ . The update rule becomes:

$$\theta_{k+1} = \theta_k - \eta \nabla_{\theta}^{\alpha}L(\theta_t) \quad (5)$$

Now computing the fractional gradient for a given  $\theta_t$  in order to derive the update rule in FASGD. For a given  $\theta_t$ , the fractional gradient is:

$$\nabla_{\theta}^{\alpha}L(\theta_t) = \frac{1}{\Gamma(1-\alpha)} \int_0^{\theta_t} \frac{\partial L(\tau)}{\partial \tau} (\theta_t - \tau)^{-\alpha} d\tau \quad (6)$$

Let  $g(\tau) = \frac{\partial L(\tau)}{\partial \tau}$ , substituting the loss function gradient eq (6) becomes:

$$\nabla_{\theta}^{\alpha}L(\theta_t) = \frac{1}{\Gamma(1-\alpha)} \int_0^{\theta_t} g(\tau) (\theta_t - \tau)^{-\alpha} d\tau \quad (7)$$

Discretizing the interval  $[0, \theta_t]$  in to  $n$  small steps of size  $\Delta\tau$ . The integral is numerically approximated as:

$$\int_0^{\theta_t} g(\tau) (\theta_t - \tau)^{-\alpha} d\tau \approx \sum_{k=0}^{n-1} g(\tau k) (\theta_t - \tau k)^{-\alpha} \Delta\tau \quad (8)$$

Where  $\tau_k = k\Delta\tau$ , the fractional gradient then becomes:

$$\nabla_{\theta}^{\alpha}L(\theta_t) \approx \frac{1}{\Gamma(1-\alpha)} \sum_{k=0}^{n-1} g(\tau k) (\theta_t - \tau k)^{-\alpha} \Delta\tau \quad (9)$$

Finally, substituting the approximate fractional gradient back in to update rule:

$$\theta_{t+1} = \theta_t - \eta \left( \frac{1}{\Gamma(1-\alpha)} \sum_{k=0}^{n-1} \frac{\partial L(\tau k)}{\partial \tau} (\theta_t - \tau k)^{-\alpha} \Delta\tau \right) \quad (10)$$

Eq (10) shows the update rule for FA-SGD depicting the integration of fractional calculus in traditional SGD to form fractionally accelerated SGD algorithm. The fractional order  $\alpha$  in fractional stochastic gradient descent (FSGD) typically

ranges between 0 and 1, while FA-SGD provides range beyond unity, when  $\alpha=1$  algorithm simplifies to traditional SGD.

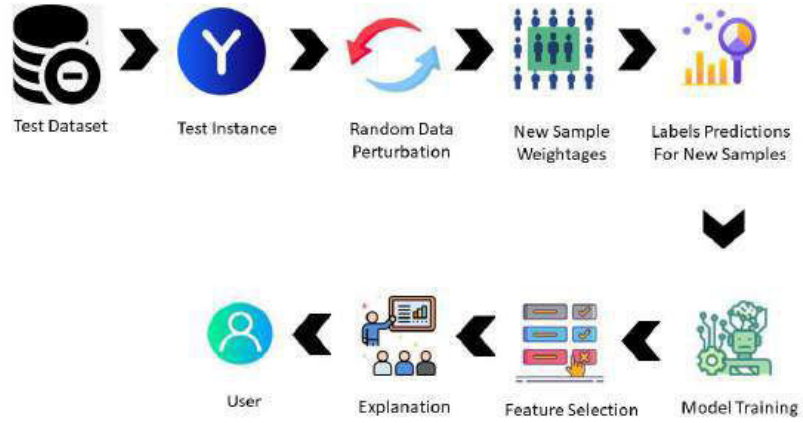


**Fig-7: Graphical Abstract of LIME**

Pseudocode for FA-SGD optimizer is given below, which assumes a modification to standard gradient decent to handle non-convex loss functions by incorporating adaptive learning rates, similar to those employed in Adam or RMSprop.

FA-SGD – Pseudocode	
<b>Input:</b>	
1. Learning rate ( $\eta$ )	
2. Momentum hyperparameter ( $\beta$ )	
3. Epsilon ( $\varepsilon$ )	
4. Fractional order ( $\alpha$ )	
5. Weight vector ( $w$ )	
6. Gradient vector ( $g$ )	
<b>Output:</b>	
• Updated weight vector	
<b>Implementation steps:</b>	
1. Initialize Learning rate, Momentum hyperparameter, Epsilon, Fractional order, Weight vector, and Gradient vector.	
2. Compute the momentum variable: $m = \beta \cdot m + g$	
3. Compute the fractional term: $\phi = ( w - previous\_w  + \delta)^{1-\alpha}$	
4. Update the weight vector ( $w$ ), using learning rate, fractional term, and momentum variable: $w = w - \eta \cdot \phi \cdot m$	
5. Update the previous weight vector ( $previous\_w = w$ )	
6. Return the updated weight vector	

**Table-4: Evaluation Metrics**

Accuracy (AC)	$\frac{trpos + trneg}{(trpos + trneg + flpos + flneg)}$
Precision (PC)	$\frac{trpos}{(trpos + flpos)}$
Recall (RC)	$\frac{trpos}{(trpos + flneg)}$
F1-Score (FS)	$2 \times \frac{PC \times RC}{PC + RC}$

### 3.8 Summary

The detailed description of the suggested ultralight CNN and FA-SGD optimization strategy is presented in this chapter, along with its derivation, by integration of “Fractional Calculus”, which transforms standard SGD to FA-SGD. Additionally Local Interpretable Model-Agnostics Explaination (LIME) is also briefly discussed.

The following chapter shows the simulation and analysis result of suggested ultralight CNN, along with the both the SGD, and FA-SGD optimization strategies.

## Chapter 4

### Simulations and Analysis

#### 4.1 Introduction

The chapter outlines the implementation of the suggested ultralight CNN for signature classification on benchmark CEDAR dataset, involving both the standard SGD and fractional calculus based FA-SGD optimization methods. The suggested model is implemented with learning rate of 0.001 and a batch size of 128 over 30 iterations after comprehensive hyperparameter optimization. Tuned parameters are applied consistently to proposed CNN model through out entire study, with sole variation being distinct alpha ( $\alpha$ ) values in each study. The results are segmented into four studies, each featuring variations in fractional order values i.e.  $\alpha$ .

#### 4.2 Study-I

Initially, the suggested ultralight CNN with optimal parameters, is implemented with SGD. Afterwards, the model is trained with FA-SGD optimization approach, by varying fractional order alpha ( $\alpha$ ) from 0.1 to 0.5 to investigate the impact of fractional order on performance criterion of ultralight CNN. The performance overall is evaluated interms of test accuracy, bias and variance. The suggested ultralight CNN shows reasonable performance with standard SGD, achieving a test accuracy of 92.1% on Test Set, alongside low bias and variance of 0.0218 and 0.3738 respectively, i.e. training and validation loss on Train and Validation sets during model's training. While FA-SGD optimization approach depicts varied performance interms of bias, variance and test accuracy for distinct alpha ( $\alpha$ ) values, achieving optimal performance at  $\alpha = 0.5$  with test accuracy of 97.2% and very low bias and variance of 0.0428 and 0.089 respectively. At  $\alpha$  value of 0.2 model shows worst performance exhibiting low bias and slightly higher variance, hence indicating the potential overfitting and

poor generalization on unseen data. Explicitly, the FA-SGD optimizer achieved accuracies ranging from 52.9% to 97.2%, with associated bias and variance ranging from 0.0428 to 0.0873 and 0.089 to 0.4137 respectively. **Table-5** provides detailed performance comparison of ultralight CNN, contrasting SGD with FA-SGD algorithm with varying  $\alpha$  values from 0.1 to 0.5. The accuracy, loss plots and confusion matrices related with study-I are presented in **Fig-[8-13]**. The results of study-I indicate that SGD model performs better than FA-SGD with  $\alpha$  values ranging up to 0.4, while only being outperformed by FA-SGD with fractional order value of 0.5, achieving highest test accuracy and very low bias and variance on training and validation sets.

### 4.3 Study-II

In this study, the suggested model is implemented with FA-SGD optimization algorithm with  $\alpha$  varying from 0.6 to 1.0, where fractional order value of 1.0 reduces FA-SGD to SGD operations. The performance of FA-SGD is further improved with  $\alpha$  values ranging from 0.6 to 1.0, reaching best test accuracy of 98% at  $\alpha=0.7$ , with associated bias and variance as low as 0.0492 and 0.0126 respectively. The FA-SGD displays exceptional performance, except for one instance at  $\alpha=0.6$ , achieving a test accuracy of merely 60.5%. The accuracies for FA-SGD with  $\alpha$  values ranging from 0.6 to 1.0 is 60.5% to 98%, while the associated bias and variance ranges span from 0.0149 to 0.0492 and 0.0126 to 0.7426 respectively. A thorough critical evaluation of the suggested ultralight CNN is tabulated in **Table-6**, with focus on its performance in conjunction with FA-SGD at  $\alpha$  values ranging from 0.6 to 1.0. The accuracy, loss plots and confusion matrices related with study-II are shown in Fig-[14-18]. The learning curves in **Fig-8** and **Fig-18** corroborate the claim that standard SGD and FA-SGD operate similarly with alpha of unity. However, it should be highlighted that FA-SGD is more effective in terms of achieving higher accuracy while minimizing bias and variance.

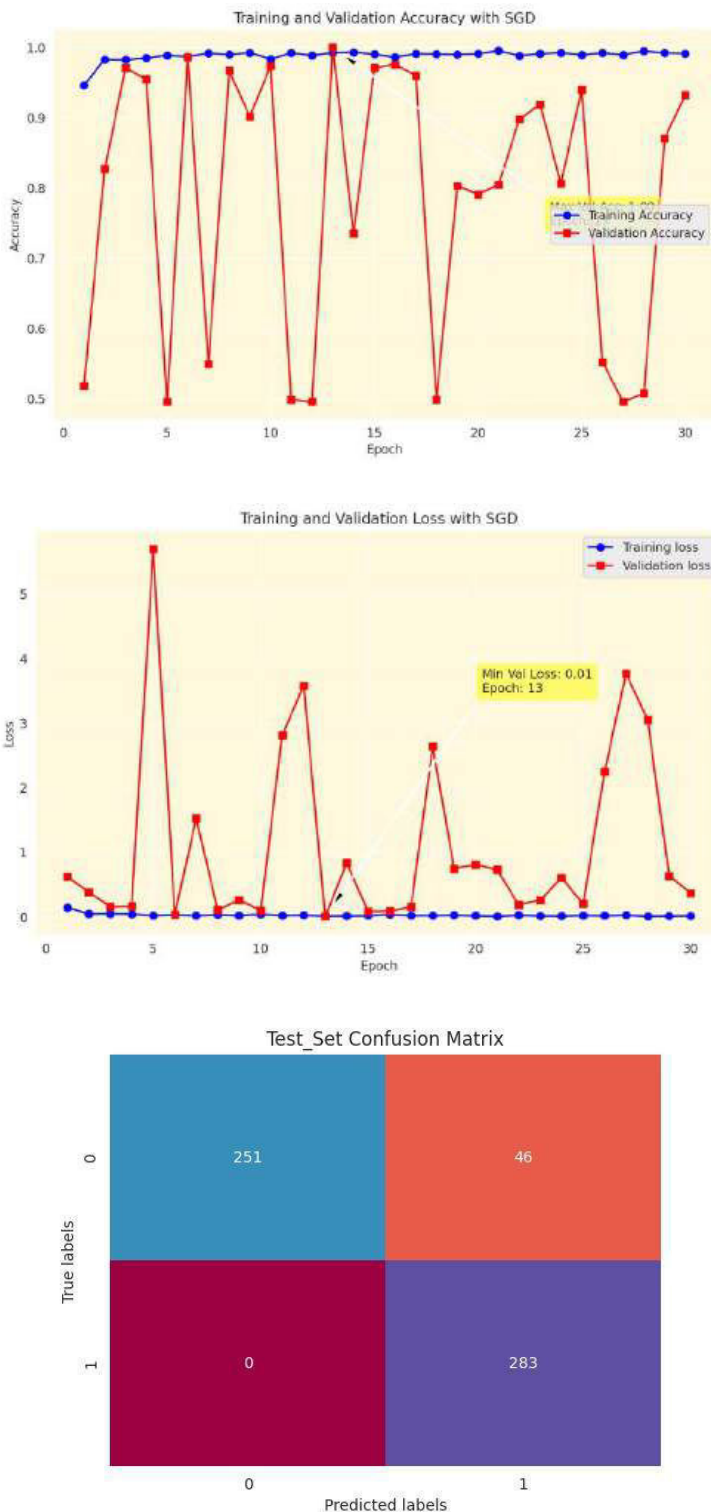


**Fig-8: Acc and Loss Plots, along with Confusion Matrix for Ultralight CNNwith SGD**

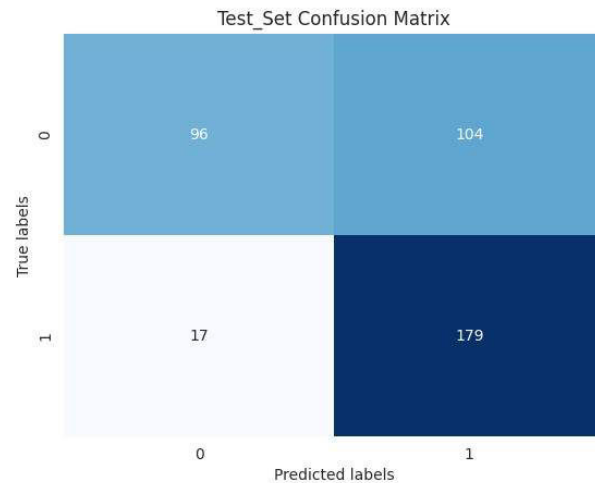
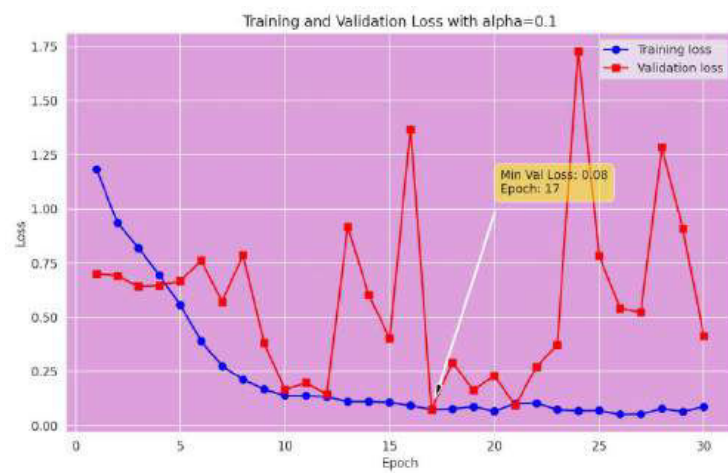
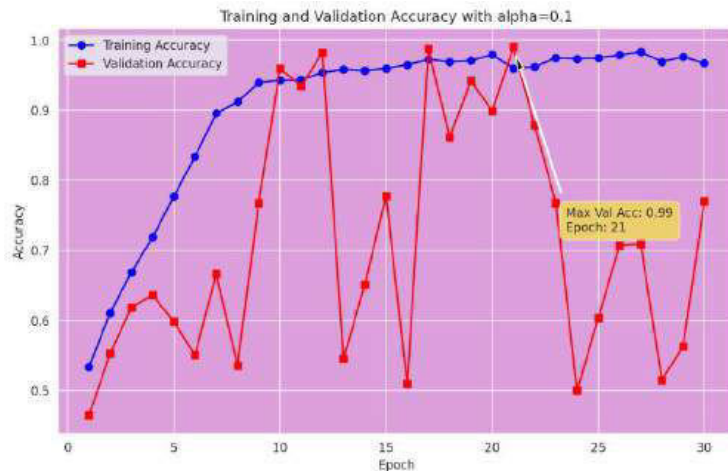


**Fig-9: Acc and Loss Plots, along with Confusion Matrix for Ultralight CNN with FA-SGD ( $\alpha=0.1$ )**

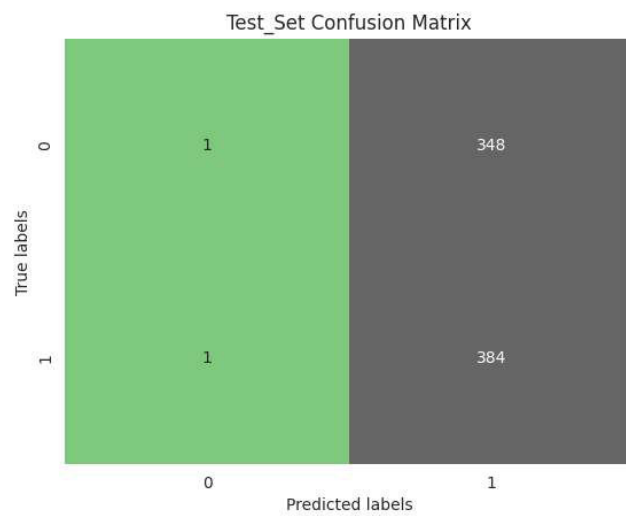
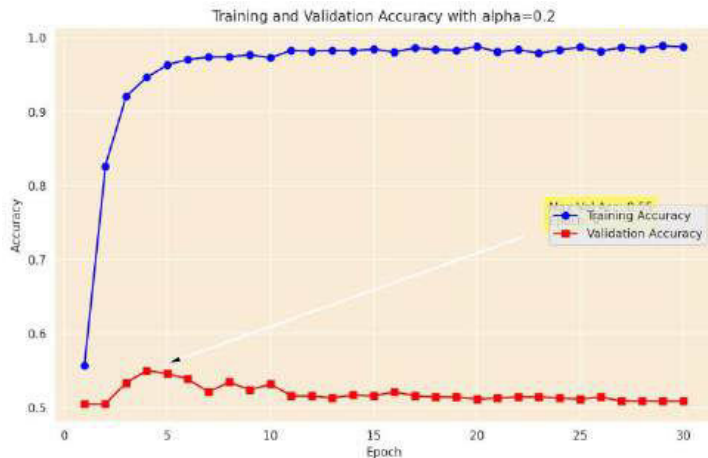


**Fig-10: Acc and Loss Plots, along with Confusion Matrix for Ultralight CNN with FA-SGD ( $\alpha = 0.2$ )**

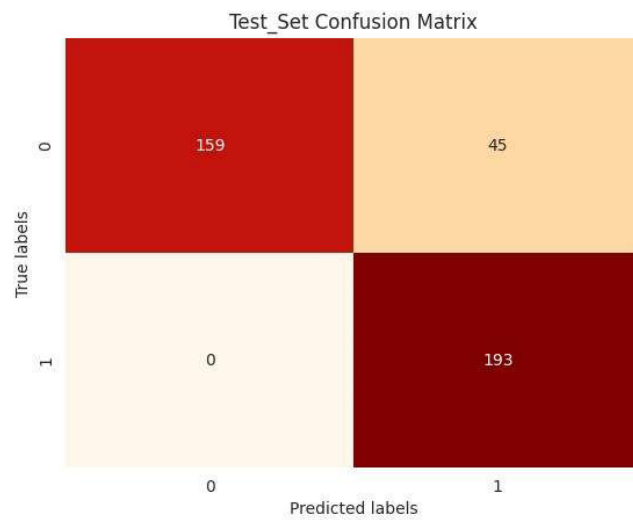
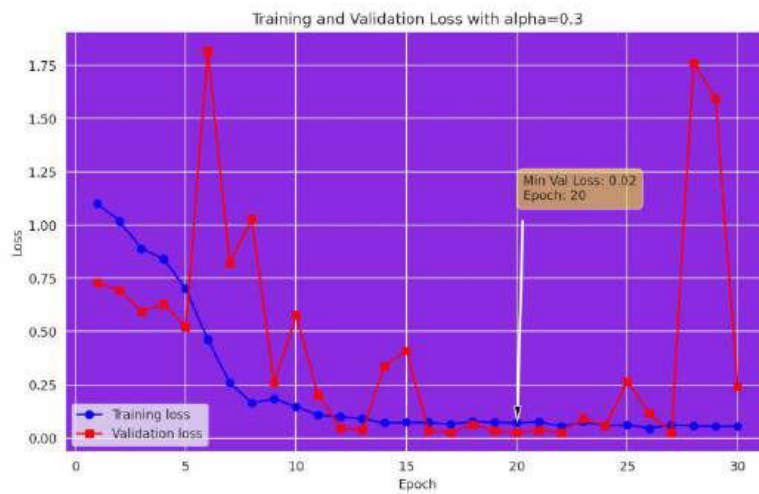
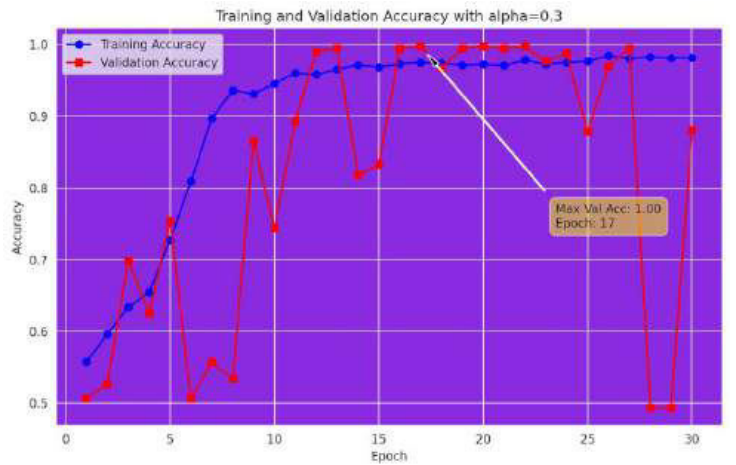


**Fig-11: Acc and Loss Plots, along with Confusion Matrix for Ultralight CNN with FA-SGD ( $\alpha = 0.3$ )**

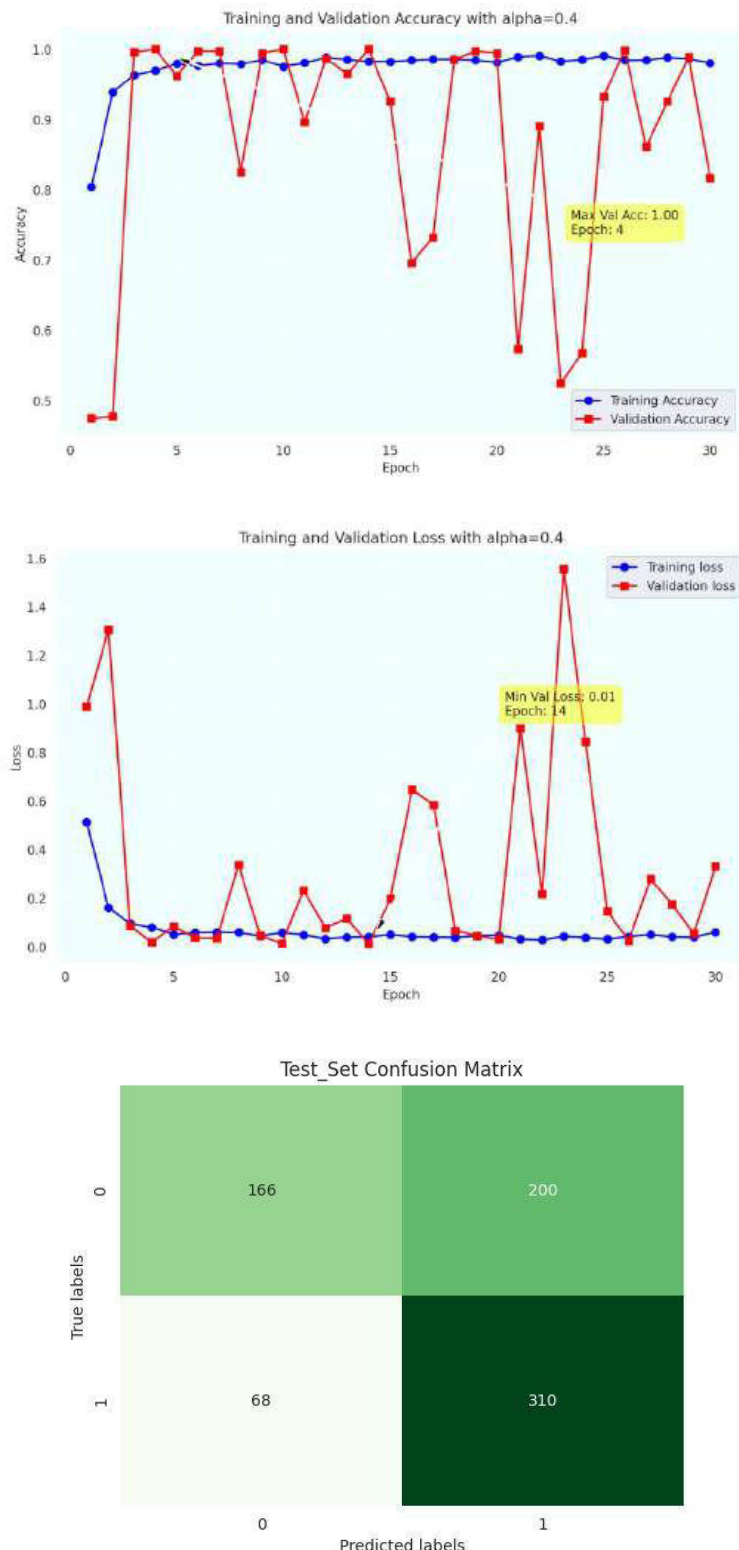


**Fig-12: Acc and Loss Plots, along with Confusion Matrix for Ultralight CNN with FA-SGD ( $\alpha = 0.4$ )**

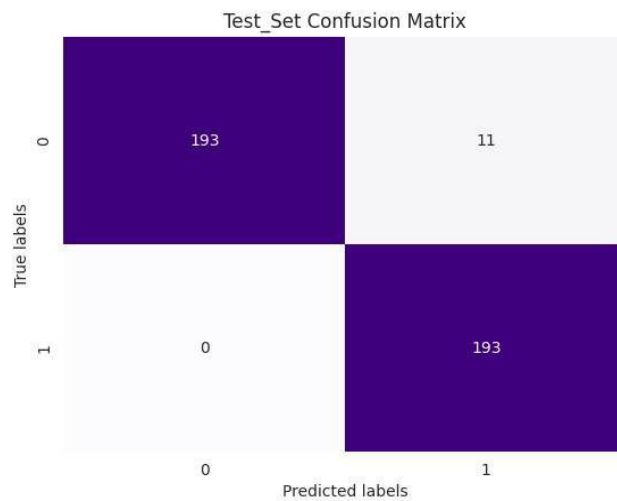
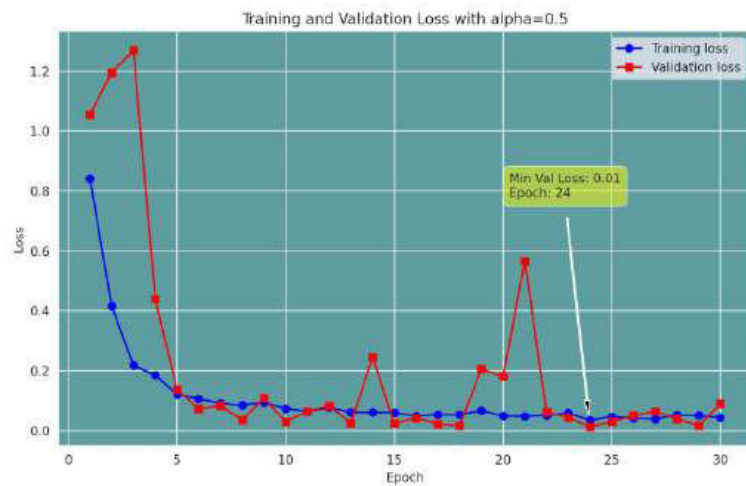
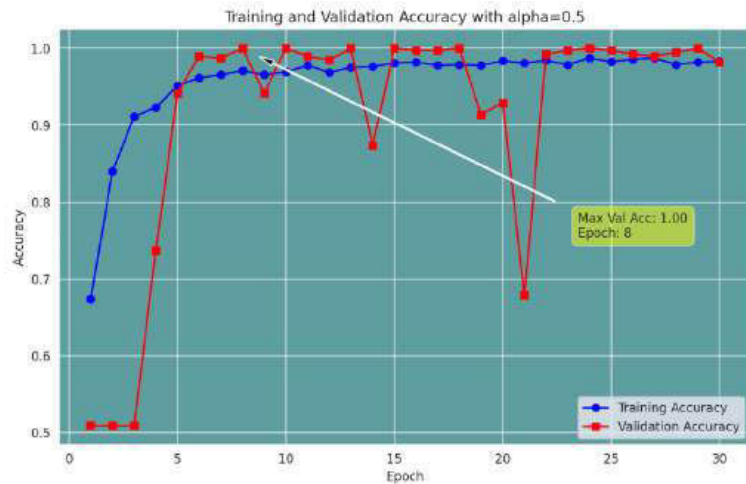


**Fig-13: Acc and Loss Plots, along with Confusion Matrix for Ultralight CNN with FA-SGD ( $\alpha = 0.5$ )**

**Table-5: Performance analysis of Study-I (Precision (PS), Recall (RC), F1-Score (FS) on test set, along with Loss (LS) and Accuracy (AC) on train, validation and test sets**

Optimizer	Label	PC, RC and FS			Training Set		Validation Set		Test Set	
		PC	RC	FS	LS	AC	LS	AC	LS	AC
SGD	Forged	1	0.85	0.92	0.021 8	95.1%	0.373 8	93.3%	0.357	92. 1%
	Genuine	0.86	1.00	0.92						
FA-SGD (alpha=0.1)	Frorged	0.85	0.48	0.61	0.087 3	86.7%	0.413 7	77%	0.398	69 %
	Genuine	0.63	0.91	0.75						
FA-SGD (alpha=0.2)	Forged	0.50	0.00	0.01	0.034 2	78.9%	1.461 4	50.9%	1.457	52. 9%
	Genuine	0.52	1.00	0.69						
FA-SGD (alpha=0.3)	Forged	1.00	0.78	0.88	0.054 6	98.2%	0.241 1	88.1%	0.231	88. 7%
	Genuine	0.81	1.00	0.90						
FA-SGD (alpha=0.4)	Forged	0.71	0.45	0.55	0.060 2	78.%	0.332 1	74.7%	0.335	64 %
	Genuine	0.61	0.82	0.70						
FA-SGD (alpha=0.5)	Forged	1.00	0.95	0.97	0.042 8	98.3%	0.089	98.2%	0.111	97. 2%
	Genuine	0.95	1.00	0.97						

**Table-6: Performance analysis of Study-II (Precision (PS), Recall (RC), F1-Score (FS) on test set, along with Loss (LS) and Accuracy (AC) on train, validation and test sets**

Optimizer	Label	PC, RC and FS			Training Set		Validation Set		Test Set	
		PC	RC	FS	LS	AC	LS	AC	LS	AC
FA-SGD (alpha=0.6)	Frorged	1.00	0.23	0.37	0.035 0	78.9%	0.742 6	60.6%	0.788	60. 5%
	Genuine	0.55	1.00	0.71						
FA-SGD (alpha=0.7)	Forged	1.00	0.97	1.00	0.049 2	98.6%	0.012 6	98.5%	0.010	98 %
	Genuine	0.97	1.00	1.00						
FA-SGD (alpha=0.8)	Forged	1.00	0.90	0.95	0.014 9	97.7%	0.139 4	94.6%	0.140	95 %
	Genuine	0.91	1.00	0.95						
FA-SGD (alpha=0.9)	Forged	1.00	0.56	0.72	0.022 9	89.1%	0.451 6	81.1%	0.473	79. 1%
	Genuine	0.71	1.00	0.83						
FA-SGD (alpha=1.0)	Forged	1.00	0.96	0.98	0.015 4	98.4%	0.139 6	98.4%	0.121	97. 9%
	Genuine	0.96	1.00	0.98						

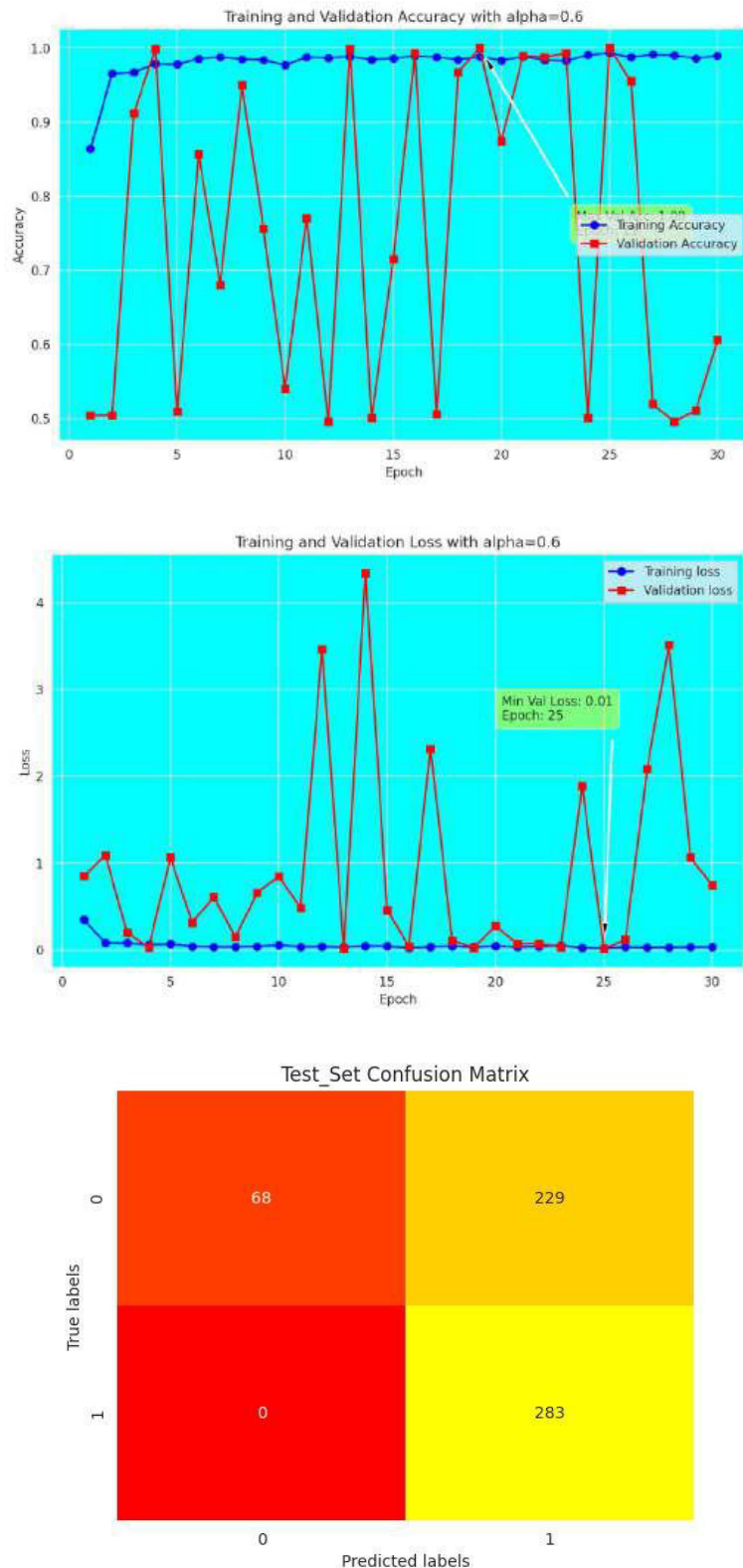


**Fig-14: Acc and Loss Plots, along with Confusion Matrix for Ultralight CNN with FA-SGD ( $\alpha = 0.6$ )**

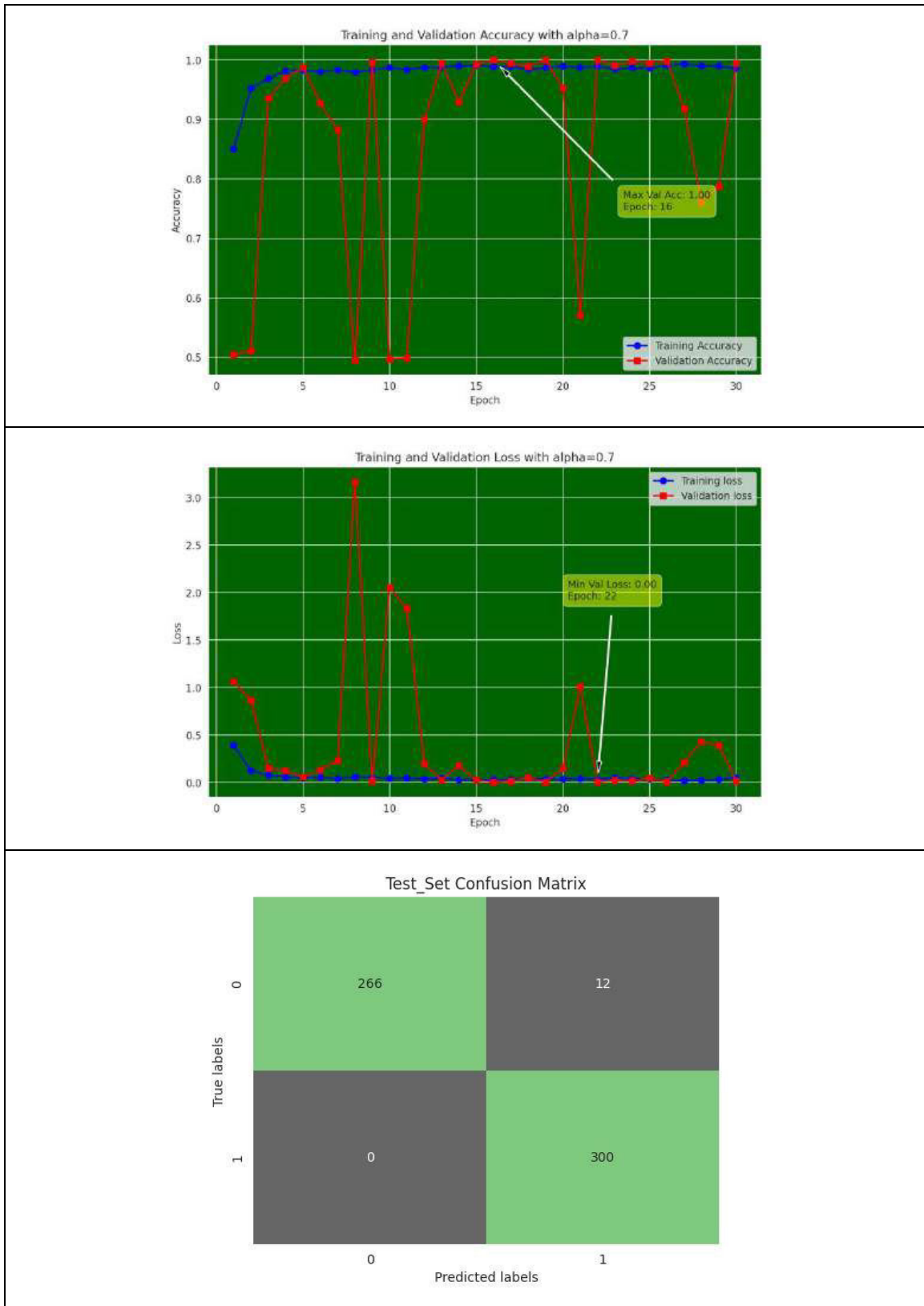


**Fig-15: Acc and Loss Plots, along with Confusion Matrix for Ultralight CNN with FA-SGD ( $\alpha = 0.7$ )**

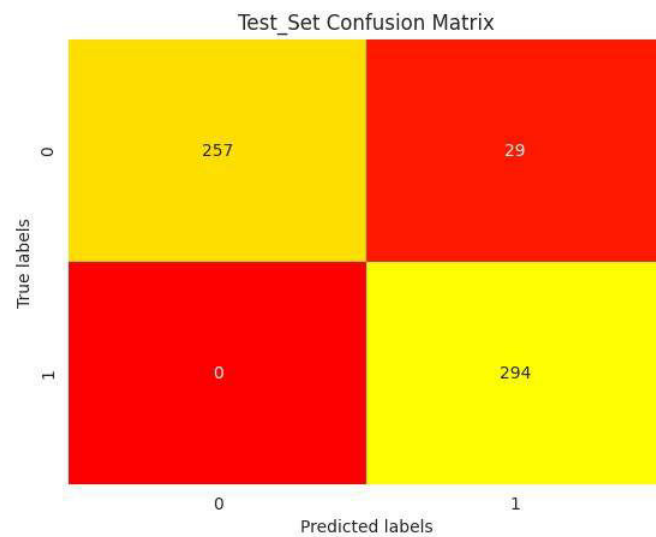
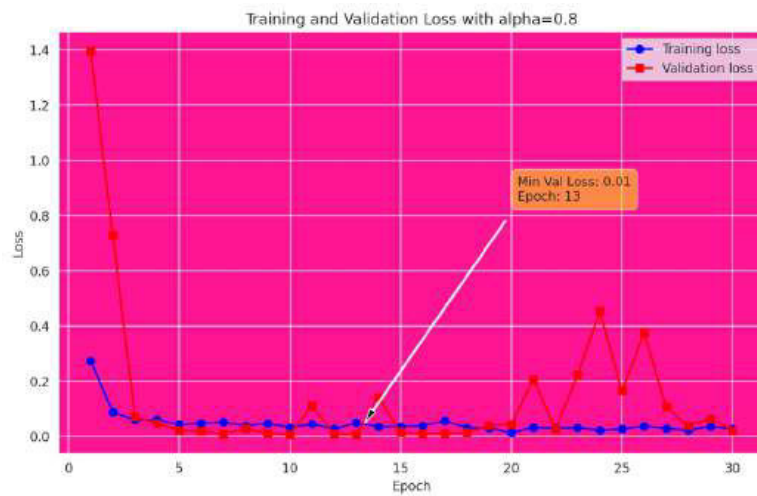
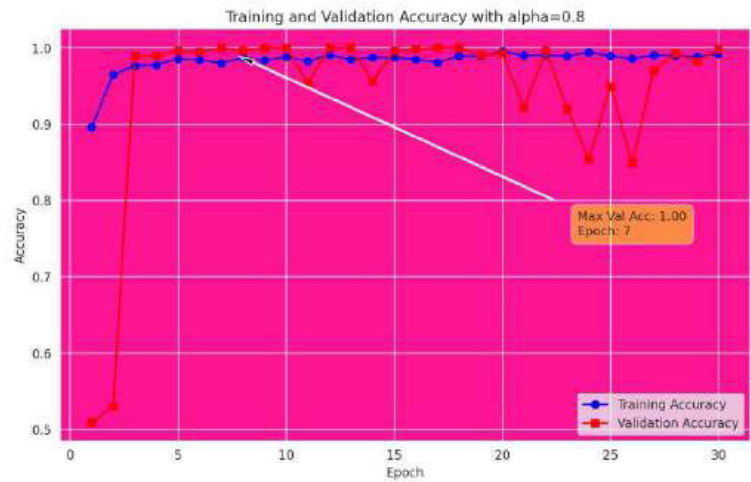


**Fig-16: Acc and Loss Plots, along with Confusion Matrix for Ultralight CNNwith FA-SGD ( $\alpha = 0.8$ )**

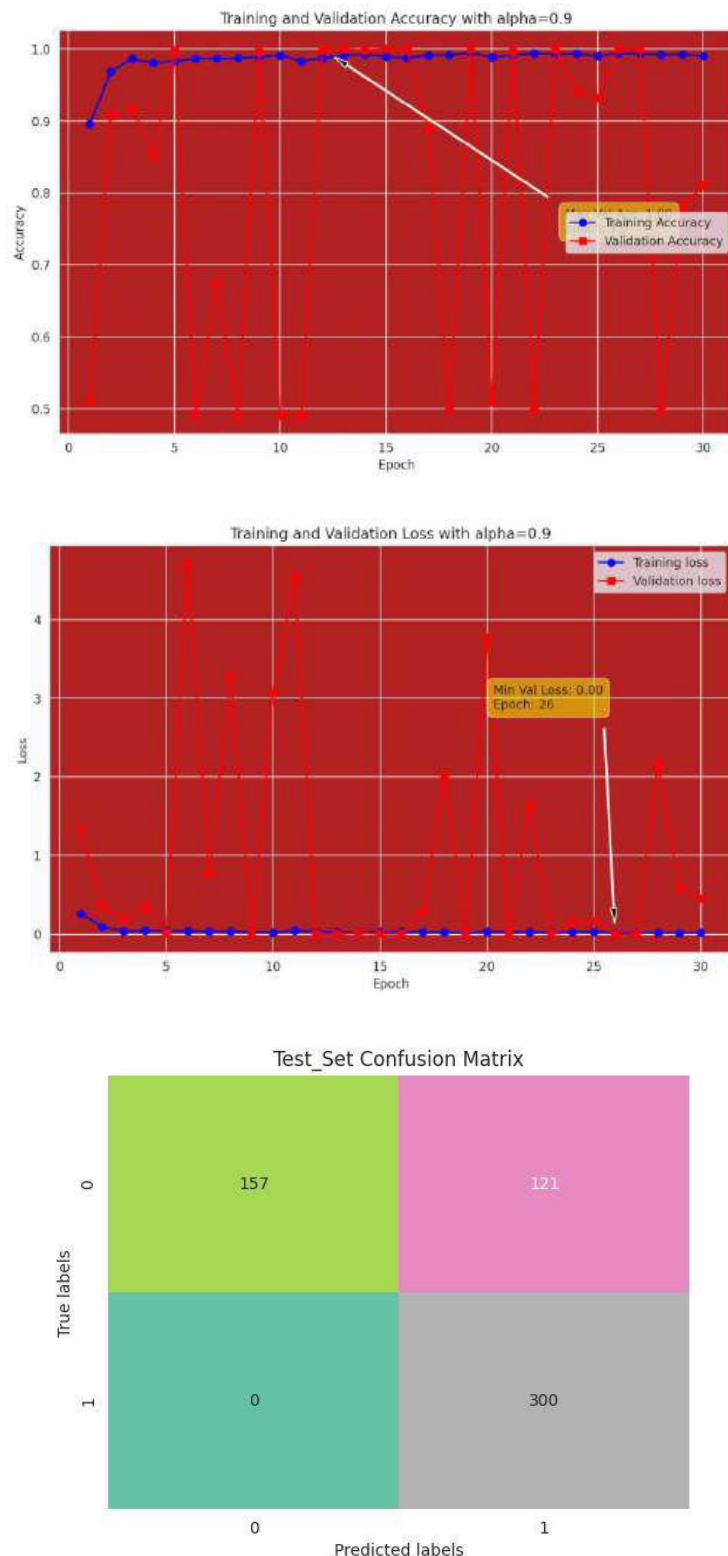


**Fig-17: Acc and Loss Plots, along with Confusion Matrix for Ultralight CNN with FA-SGD ( $\alpha = 0.9$ )**

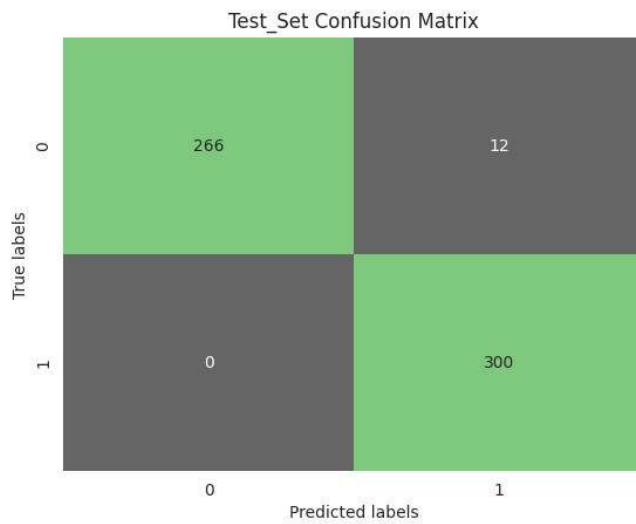
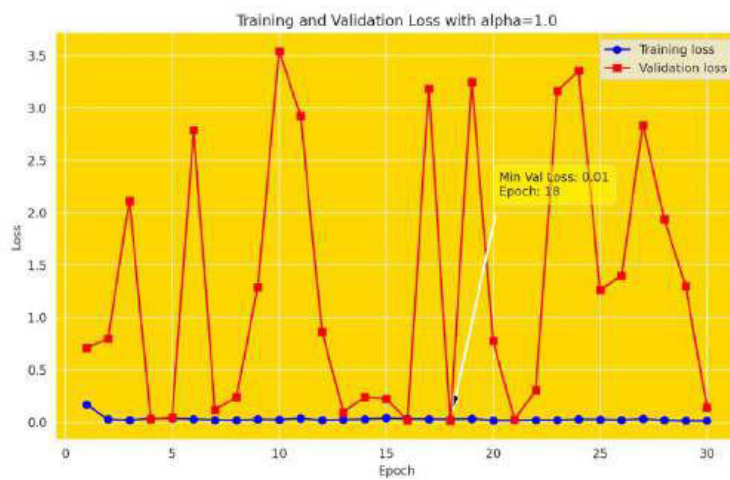
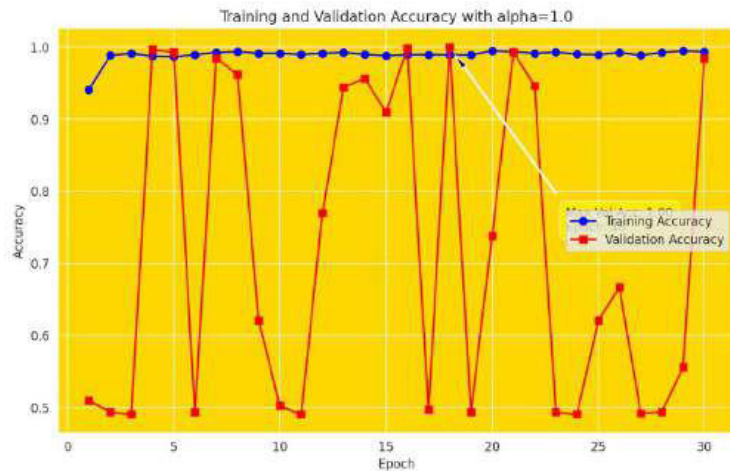


**Fig-18: Acc and Loss Plots, along with Confusion Matrix for Ultralight CNNwith FA-SGD ( $\alpha = 1.0$ )**

#### 4.4 Study-III

Study-III, presents the performance of ultralight CNN with  $\alpha$  value beyond unity, ranging up to 1.5. **Table-7** provides detailed performance assessment of suggested CNN with  $\alpha$  values ranging from 1.1 to 1.5. Accuracy range for the suggested model with  $\alpha$  value varying from 1.1 to 1.5 span from 52.2% to 97.9%, while the associated bias and variance range span from 0.0089 to 0.0156 and 0.1394 to 2.2135 respectively, as tabulated in **Table-7**. The accuracy, loss plots and confusion matrix affiliated with Study-III are displayed in **Fig-[19-23]**. Optimal performance is achieved by the suggested model with fractional order value of 1.3, attaining a generalized accuracy of 97.9%, bias and variance of 0.0097 and 0.2240. Overall, the model displays below average performance with fractional order alpha ranging from 1.1 to 1.5 except two instances, at alpha values of 1.3 and 1.5, where it converges to test accuracy above 90%.

#### 4.5 Study-IV

Finally, the suggested ultralight CNN is implemented with  $\alpha$  values spanning from 1.6 to 1.9. **Table-8** depicts the performance assessment of ultralight CNN with FA-SGD optimizer, varying the fractional order alpha from 1.6 to 1.9. From **Table-8** it is evident that the suggested CNN performs worst with alpha values ranging from 1.6 to 1.9, not converging to even 60% accuracy in a single instance, and exhibiting very high biases and variances. Test accuracy range span from 48.2% to 55.3% for  $\alpha$  values of 1.6 to 1.9, whereas bias and variance range span from 0.0192 to 11.3214 and 2.4658 to 4.9981 respectively, which can be inferred from **Table-8**. The accuracy, loss plots and confusion matrix associated with Study-IV are presented in **Fig-[24-27]**. After the comprehensive analysis of ultralight CNN with FA-SGD optimization approach across fractional order variations, it is determined that the most favourable outcomes occur with alpha rate of 0.7, achieving best test accuracy of 100% for classification of handwritten signature images using benchmark CEDAR dataset.

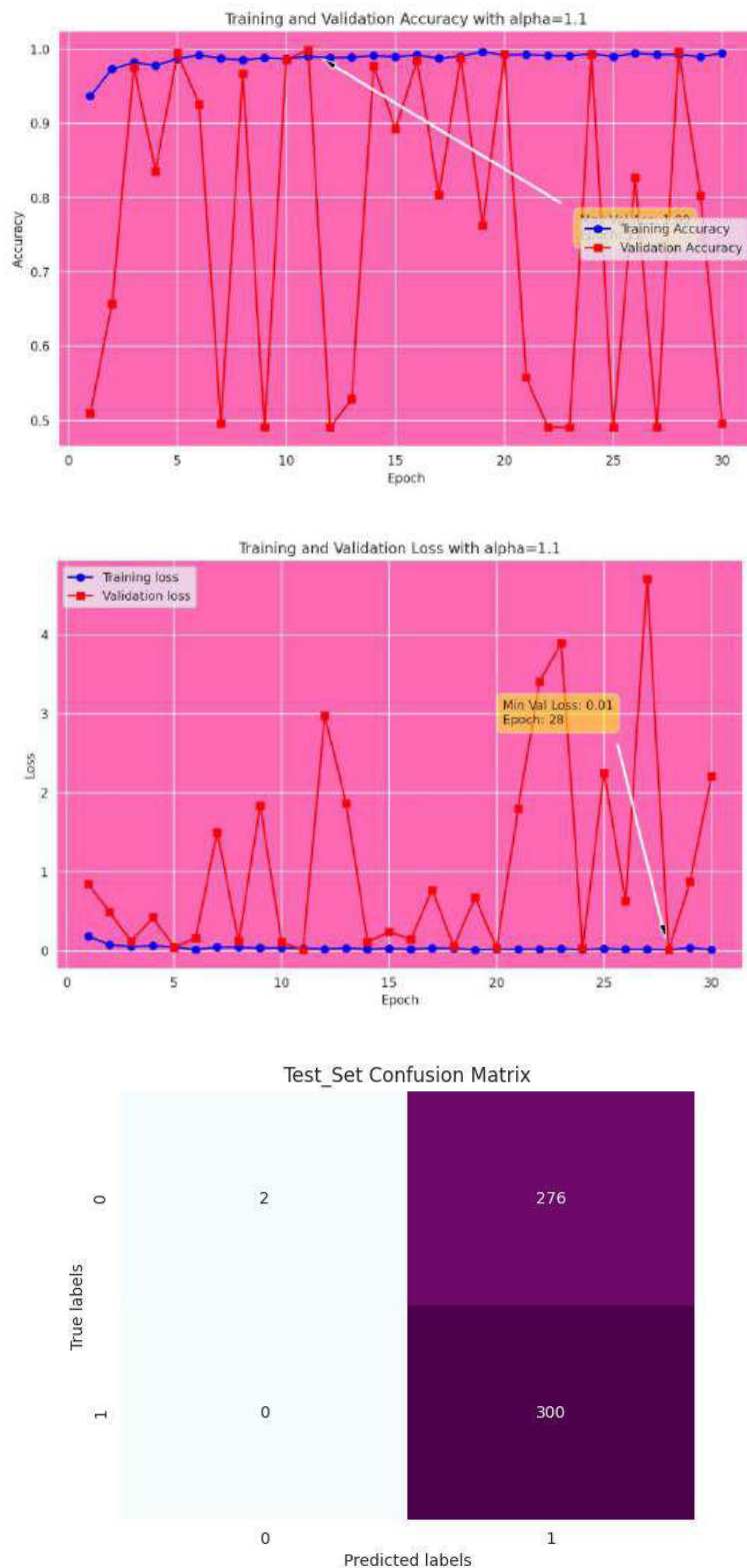


**Fig-19: Acc and Loss Plots, along with Confusion Matrix for Ultralight CNNwith FA-SGD ( $\alpha = 1.1$ )**

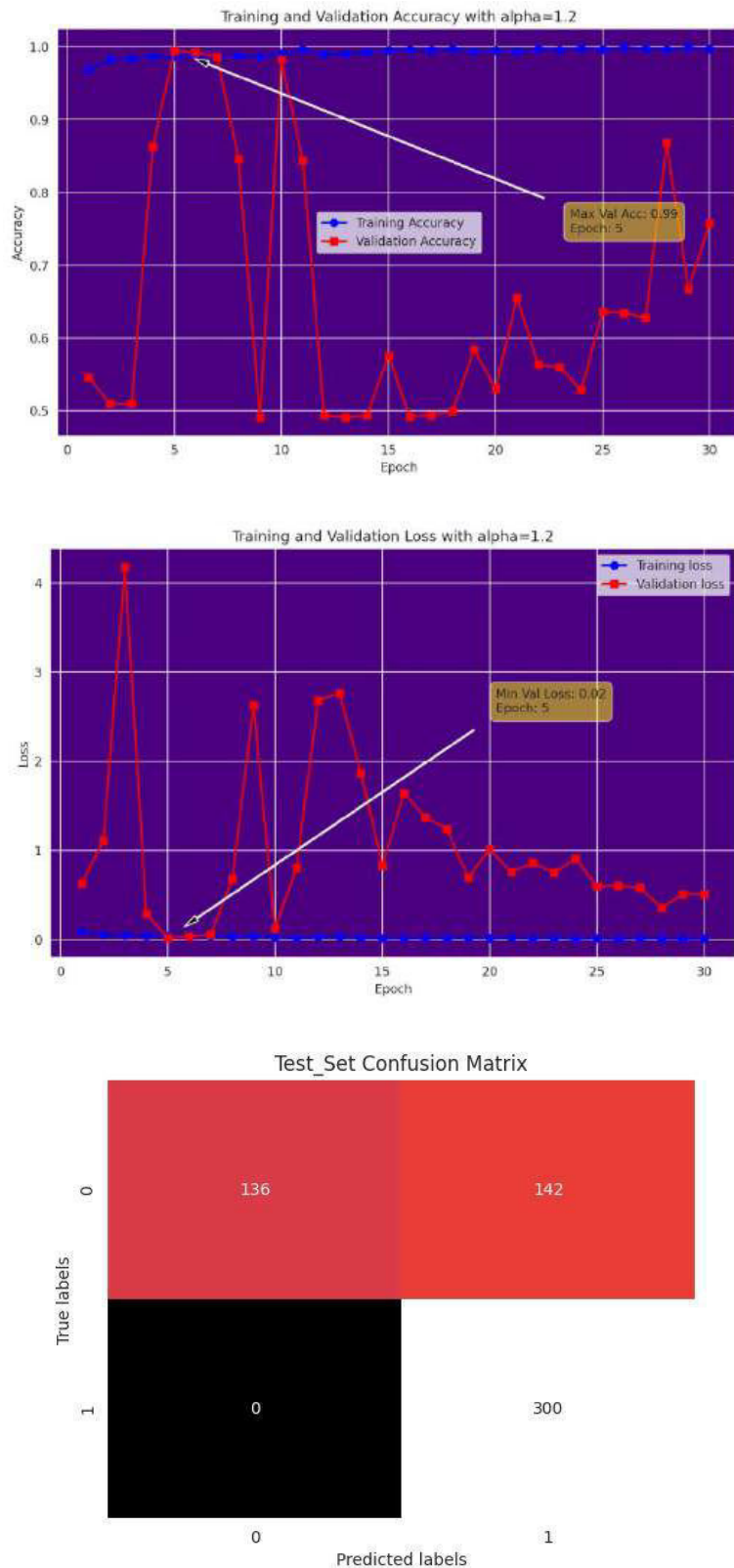


**Fig-20: Acc and Loss Plots, along with Confusion Matrix for Ultralight CNN with FA-SGD ( $\alpha = 1.2$ )**

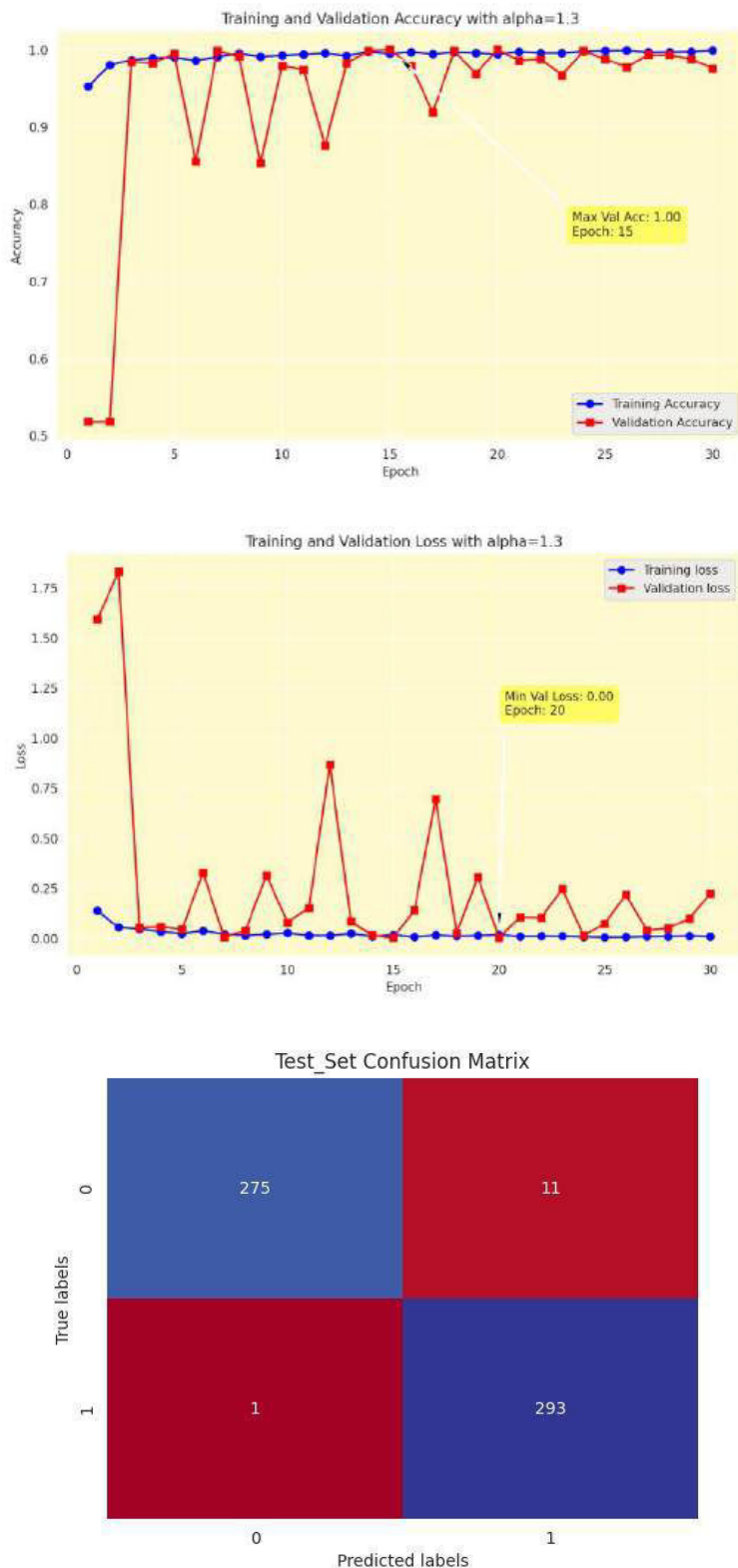


**Fig-21: Acc and Loss Plots, along with Confusion Matrix for Ultralight CNN with FA-SGD ( $\alpha=1.3$ )**

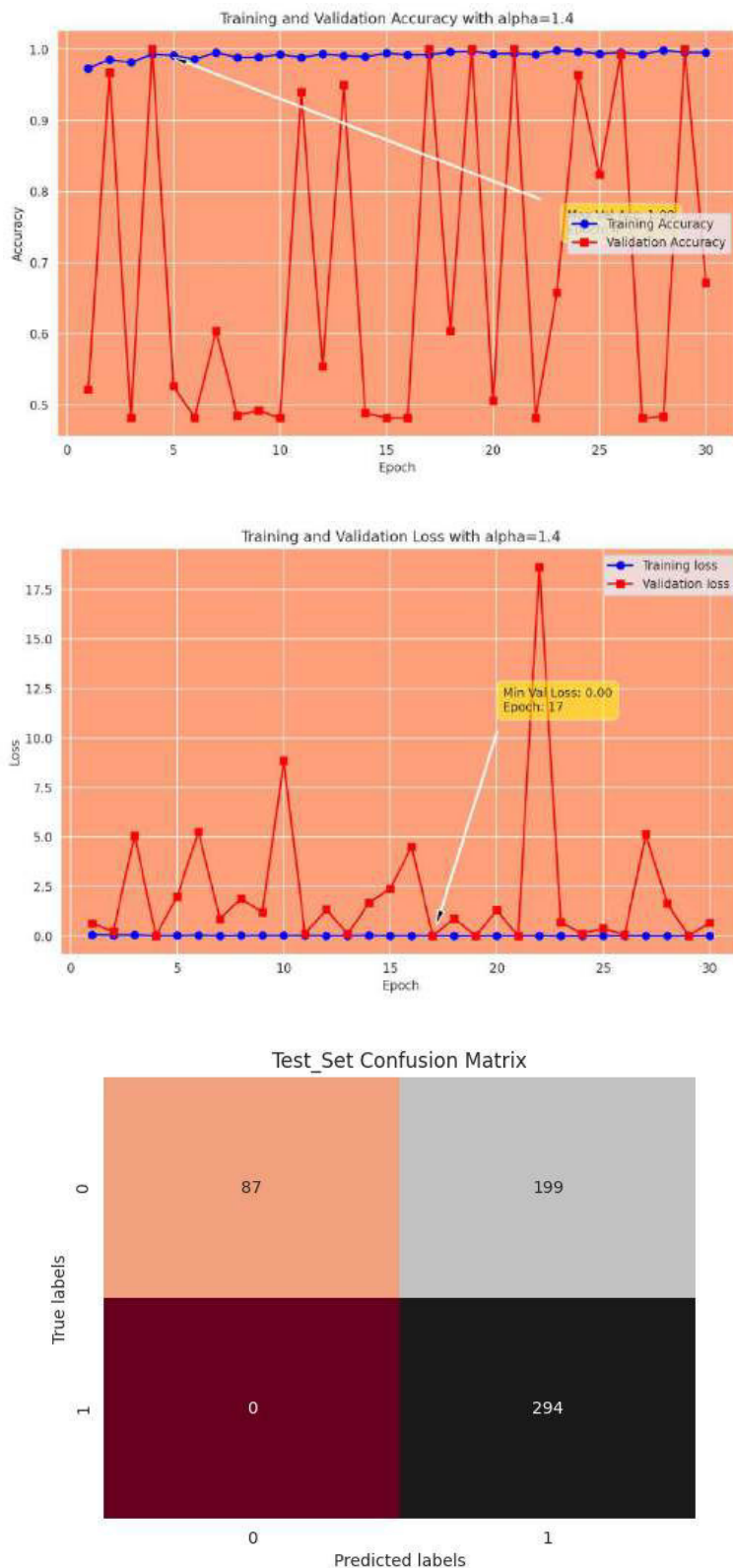


**Fig-22: Acc and Loss Plots, along with Confusion Matrix for Ultralight CNN with FA-SGD ( $\alpha = 1.4$ )**

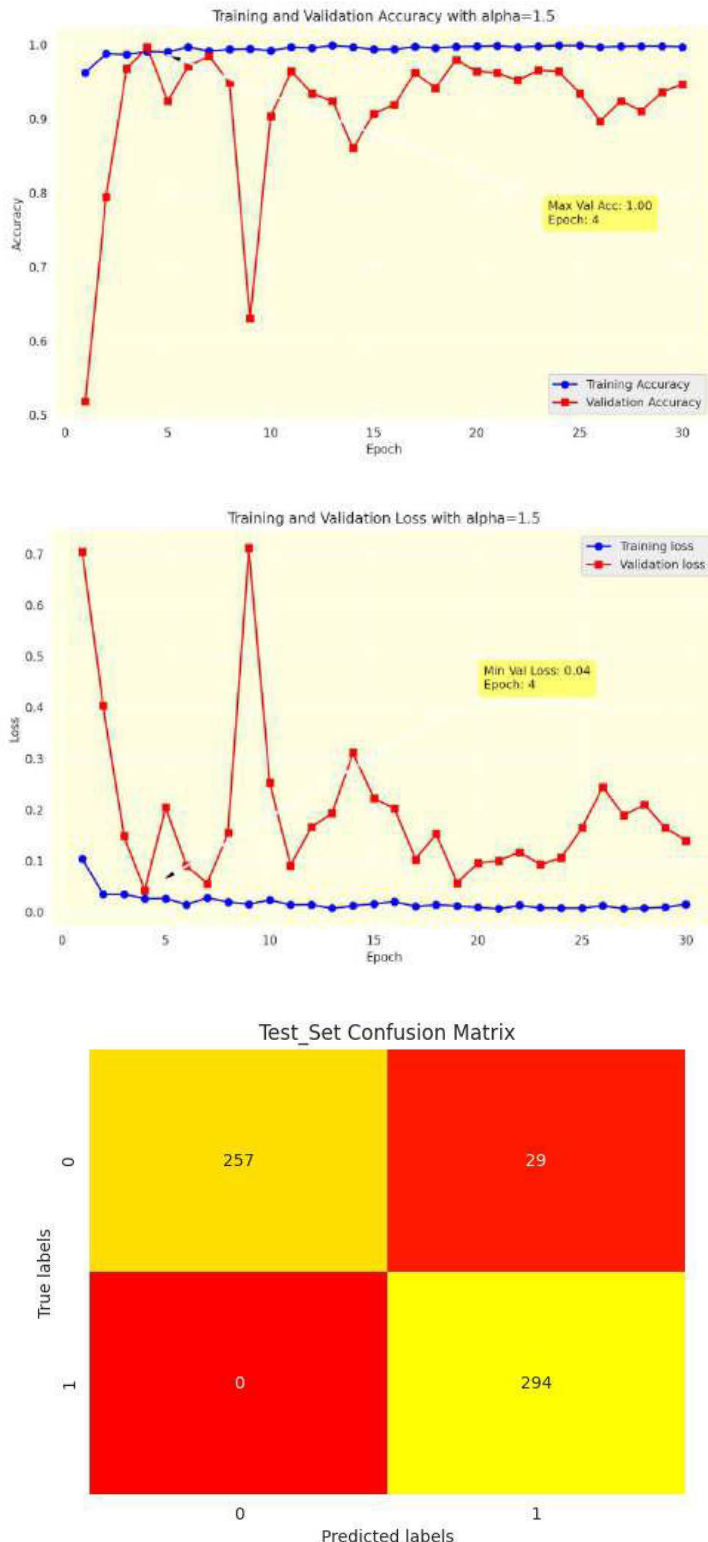


**Fig-23: Acc and Loss Plots, along with Confusion Matrix for Ultralight CNN with FA-SGD ( $\alpha = 1.5$ )**

**Table-7: Performance analysis of Study-III (Precision (PS), Recall (RC), F1-Score (FS) on test set, along with Loss (LS) and Accuracy (AC) on train, validation and test sets**

Optimizer	Label	PC, RC and FS			Training Set		Validation Set		Test Set	
		PC	RC	FS	LS	AC	LS	AC	LS	AC
FA-SGD (alpha=1.1)	Forged	1.00	0.01	0.01	0.0156	99.4%	2.2135	49.6%	2.103	52.2 %
	Genuine	0.52	1.00	0.68						
FA-SGD (alpha=1.2)	Forged	1.00	0.49	0.66	0.0089	99.7%	0.5095	75.7%	0.450	75.4 %
	Genuine	0.68	1.00	0.81						
FA-SGD (alpha=1.3)	Forged	1.00	0.96	0.98	0.0097	99.9%	0.2240	97.6%	0.156	97.9 %
	Genuine	0.96	1.00	0.98						
FA-SGD (alpha=1.4)	Forged	1.00	0.30	0.47	0.0137	99.6%	0.6678	67.2%	0.639	65.7 %
	Genuine	0.60	1.00	0.75						
FA-SGD (alpha=1.5)	Forged	1.00	0.90	0.95	0.0149	99.7%	0.1394	94.6%	0.140	95%
	Genuine	0.91	1.00	0.95						

**Table-8: Performance analysis of Study-IV (Precision (PS), Recall (RC), F1-Score (FS) on test set, along with Loss (LS) and Accuracy (AC) on train, validation and test sets**

Optimizer	Label	PC, RC and FS			Training set		Validation Set		Test Set	
		PC	RC	FS	LS	AC	LS	AC	LS	AC
FA-SGD (alpha=1.6)	Forged	0.00	0.00	0.00	0.0192	99.4 %	4.998	49. 1	4.761	50.7 %
	Genuine	0.51	1.00	0.67						
FA-SGD (alpha=1.7)	Forged	1.00	0.07	0.13	1.5942	55.5 %	2.465	51. 8	2.351	55.2 %
	Genuine	0.54	1.00	0.70						
FA-SGD (alpha=1.8)	Forged	0.00	0.00	0.00	11.321	49.9 %	3.301	50. 1	3.432	48.2 %
	Genuine	0.48	1.00	0.65						
FA-SGD (alpha=1.9)	Forged	0.50	1.00	0.67	7.7622	50.2 %	2.750	50. 7	2.783	50.2 %
	Genuine	0.00	0.00	0.00						



**Fig-24: Acc and Loss Plots, along with Confusion Matrix for Ultralight CNN with FA-SGD ( $\alpha = 1.6$ )**

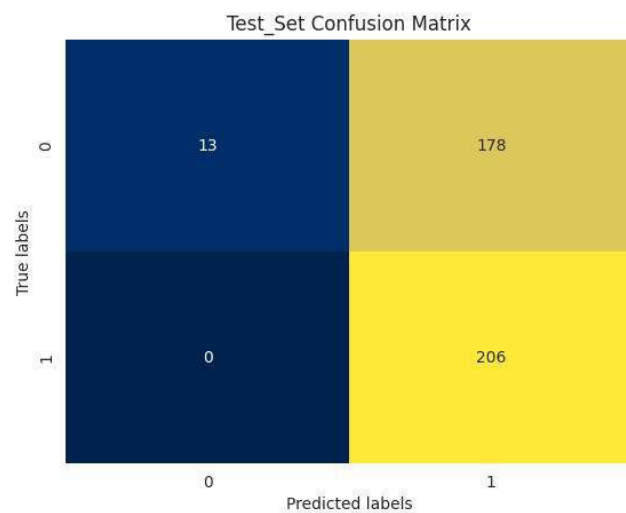
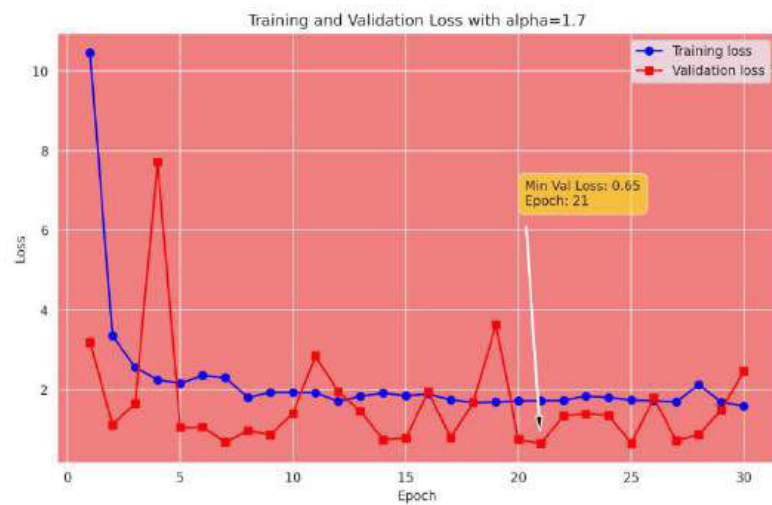
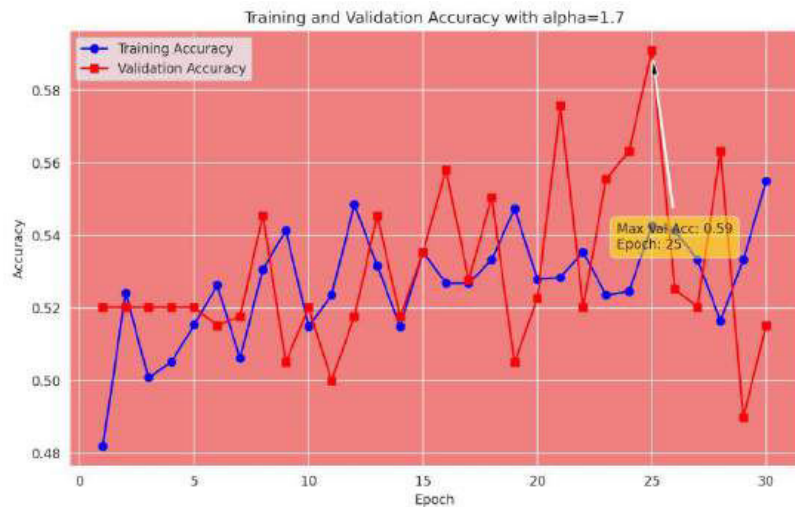


**Fig-25: Acc and Loss Plots, along with Confusion Matrix for Ultralight CNN with FA-SGD ( $\alpha=1.7$ )**

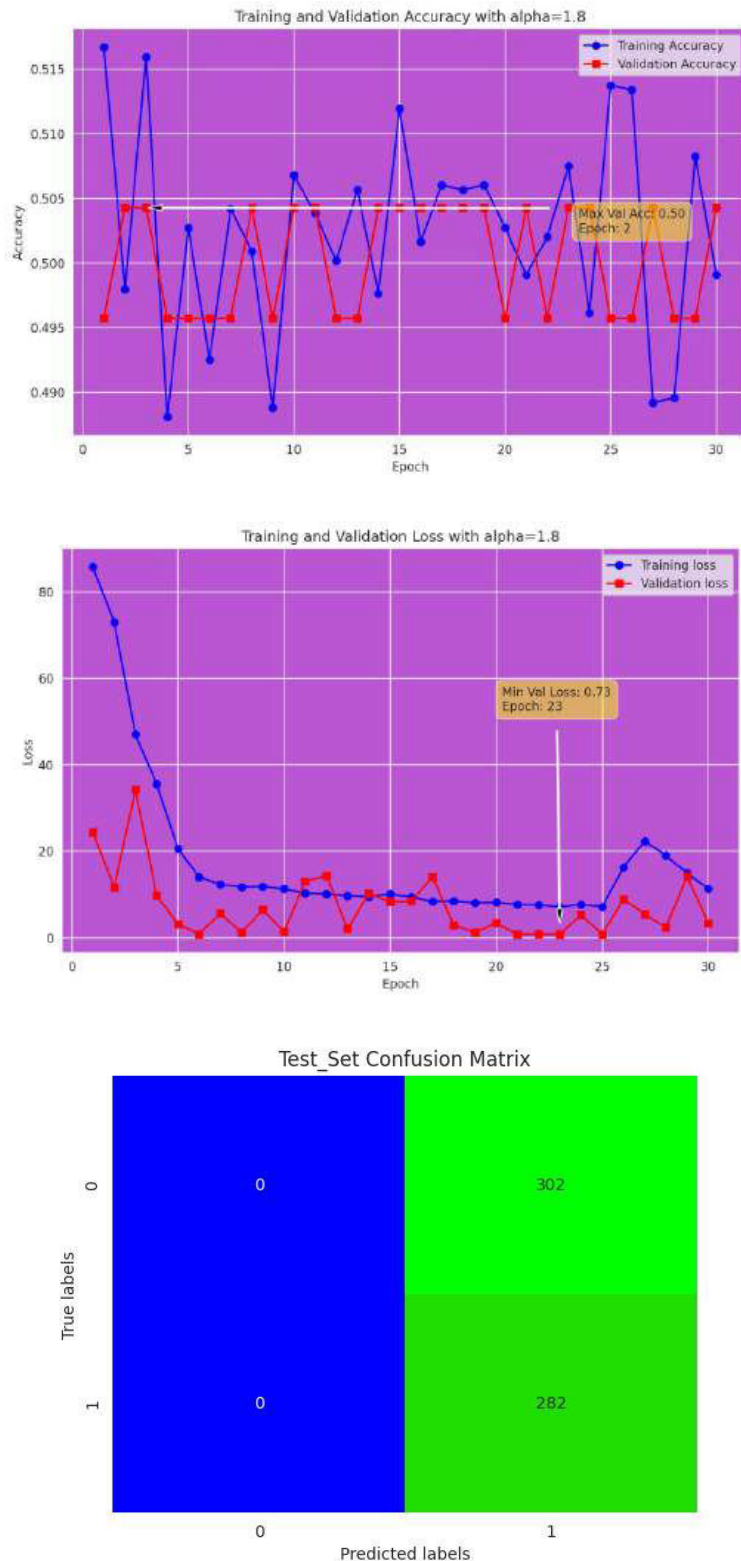


**Fig-26: Acc and Loss Plots, along with Confusion Matrix for Ultralight CNN with FA-SGD ( $\alpha = 1.8$ )**

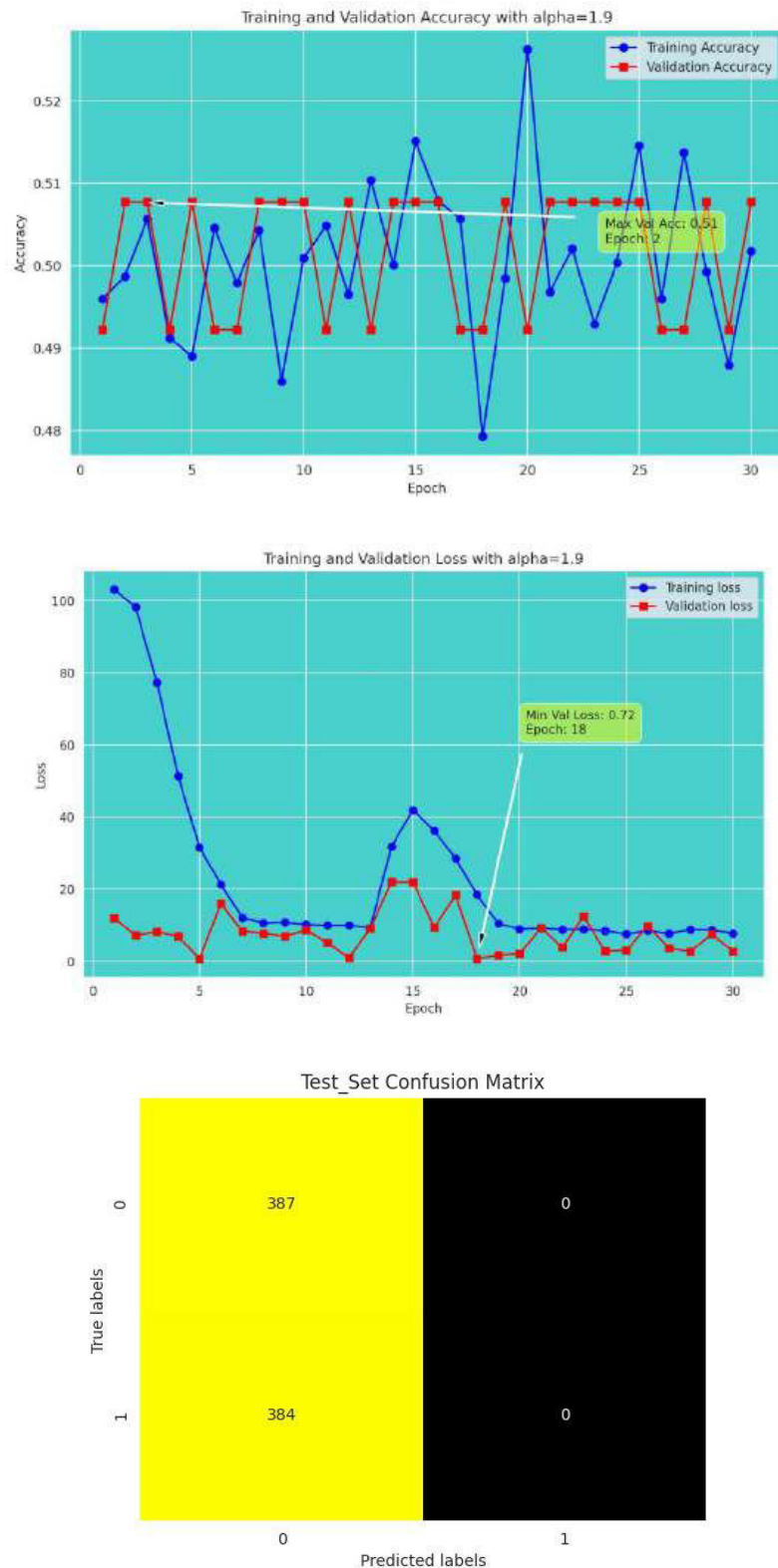


**Fig-27: Acc and Loss Plots, along with Confusion Matrix for Ultralight CNN with FA-SGD ( $\alpha=1.9$ )**

## 4.6 Discussion

This study addresses challenge of signature verification by combining ultralight CNN model with novel FA-SGD optimization algorithm. Following a thorough performance investigation of the suggested model using standard SGD and novel FA-SGD optimization strategy, it can be inferred that Ultralight CNN model coupled with FA-SGD achieves best test accuracy of 98% with low bias and variance at  $\alpha$  value of 0.7. The best computed hyperparameters are incorporated after extensive hyperparameter tuning to execute lightweight CNN model with above-mentioned optimization strategies which include SGD and FA-SGD with varying alpha on the benchmark CEDAR dataset. Combined learning cuve for each study, focusing on model's loss and accuracy is illustrated in **Fig-[28-43]**.

## 4.7 Comparison with existing Benchmark Models

The suggested CNN model demonstrates exceptional performance to accurately classify genuine and forged signatures. The comparison of the suggested ultralight model with existing benchmark models interms of test accuracy on benchmark CEDAR dataset is tabulated in **Table-9**. The performance comparison demonstrates that the proposed lightweight model based on novel FA-SGD optimization strategy outperforms existing SOTA models on benchmark CEDAR database interms of test accuracy, computational efficiency and interpretability.

**Table-9: Comparative Analysis with existing benchmark models on CEDAR database**

Authors	Technique	Accuracy(%)
[44]	Inverse Discriminative Network (IDN)	95.32
[49]	CNN + HOG + LSTM	93.7
	CNN + HOG + KNN	91.3
	CNN + HOG + SVM	94.1
[60]	FC-ResNet	96.21
[61]	VGG-16 + One Class Support Vector Machine (OC-SVM)	91.3
<b>Proposed</b>	<b>Lightweight CNN + FA-SGD</b>	<b>98</b>

#### 4.8 Predictive Strength

The proposed approach accurately distinguishes between signatures and forgeries, thus demonstrating substantial predictive capabilities. Transparency is very essential to ensure trust and reliability in biometric domain, hence this study employs LIME to offer insights into the decision making process of the suggested Ultralight model for verification of handwritten signatures. Basically the LIME approach decodes decision making process of ML models by highlighting important features in image. By critically visualizing the highlighted portions of the image, it becomes evident that which region is essential for accurate classification. **Fig-32** depicts few predictions made by the suggested ultralight CNN model and the subsequent interpretable explanations generated by LIME on unseen images of CEDAR dataset.

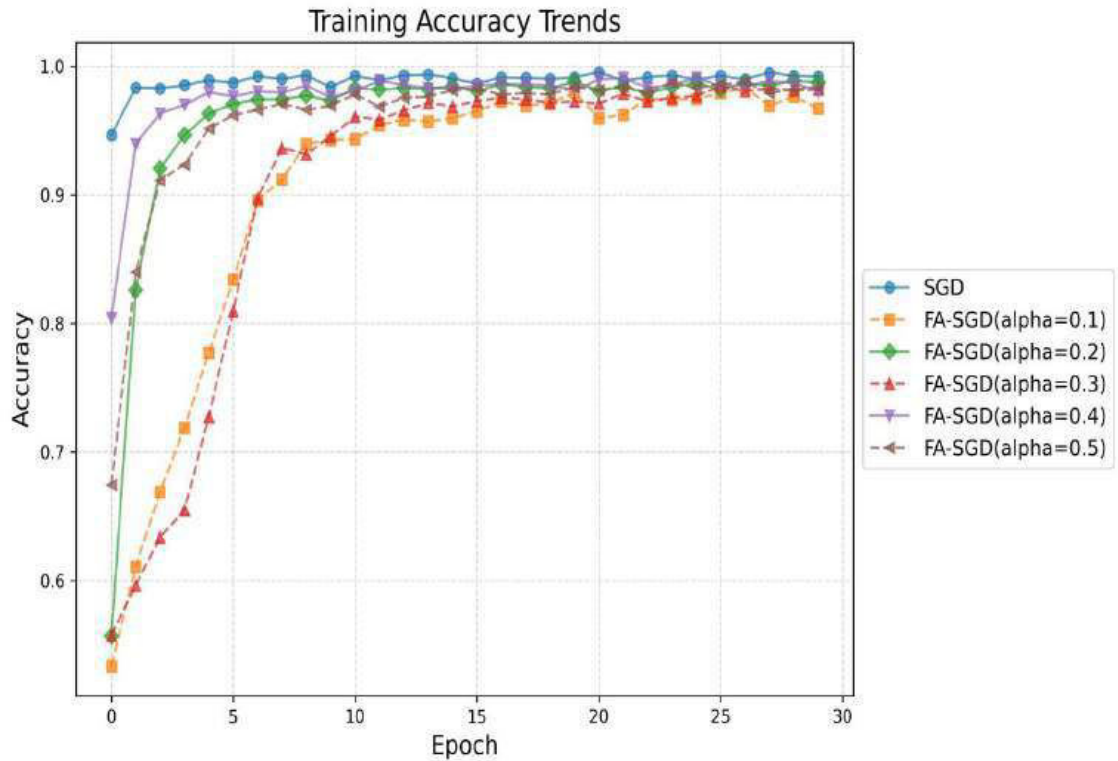


**Fig-28: Combined Learning Curve visualization of training accuracy trends for Study-I**

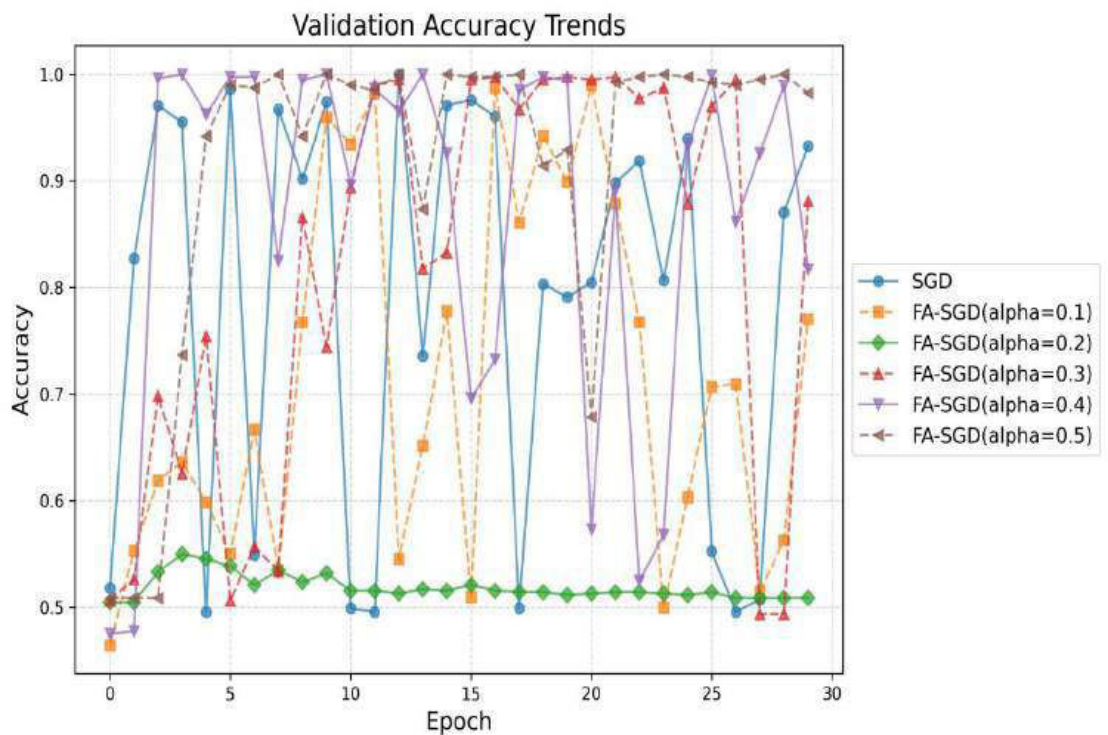


**Fig-29: Combined Learning Curve visualization of validation accuracy trends for Study-I**

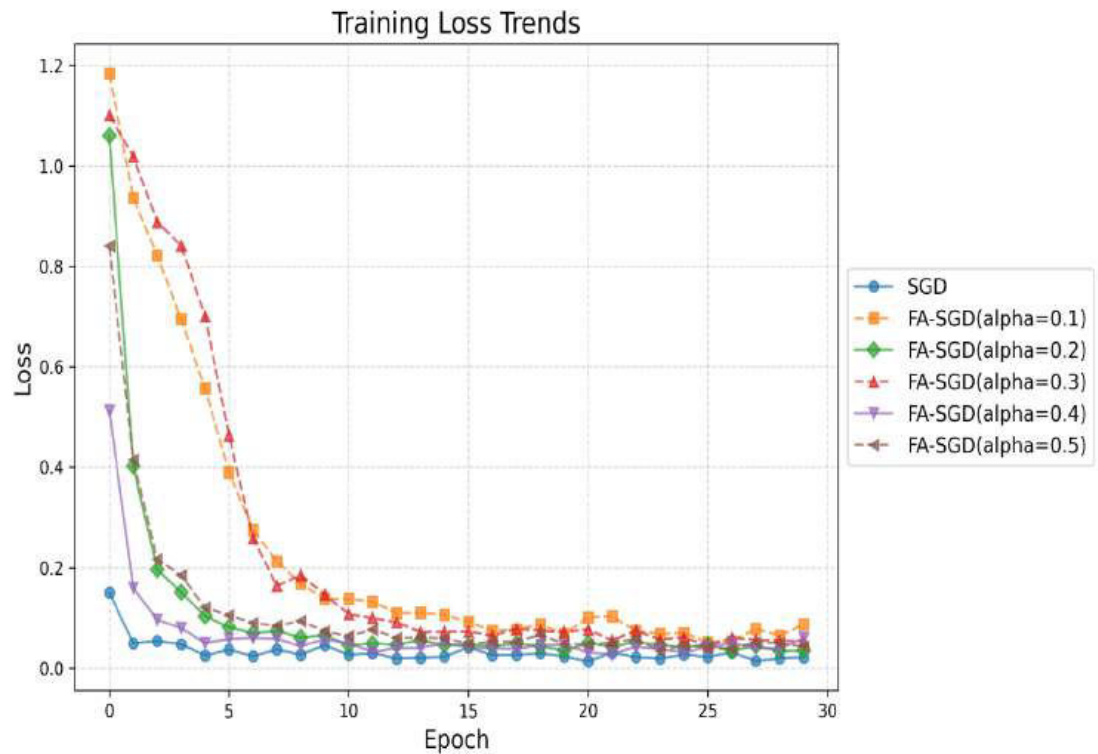


**Fig-30: Combined Learning Curve visualization of training loss trends for Study-I**

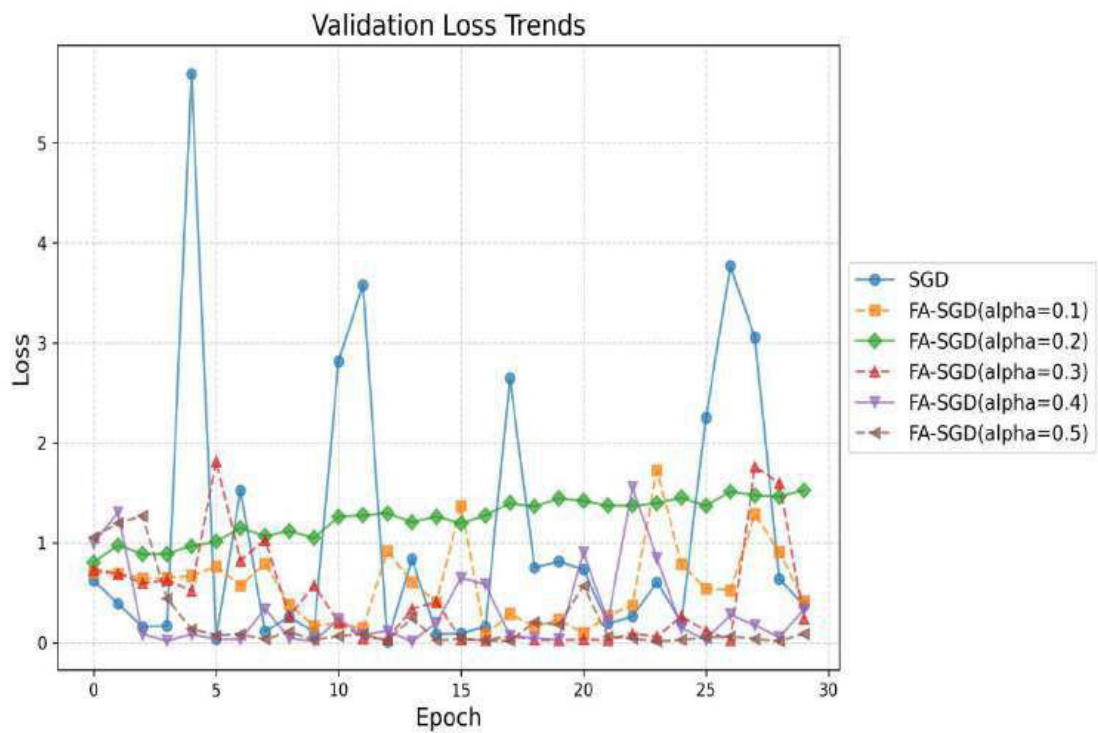


**Fig-31: Combined Learning Curve visualization of validation loss trends for Study-I**

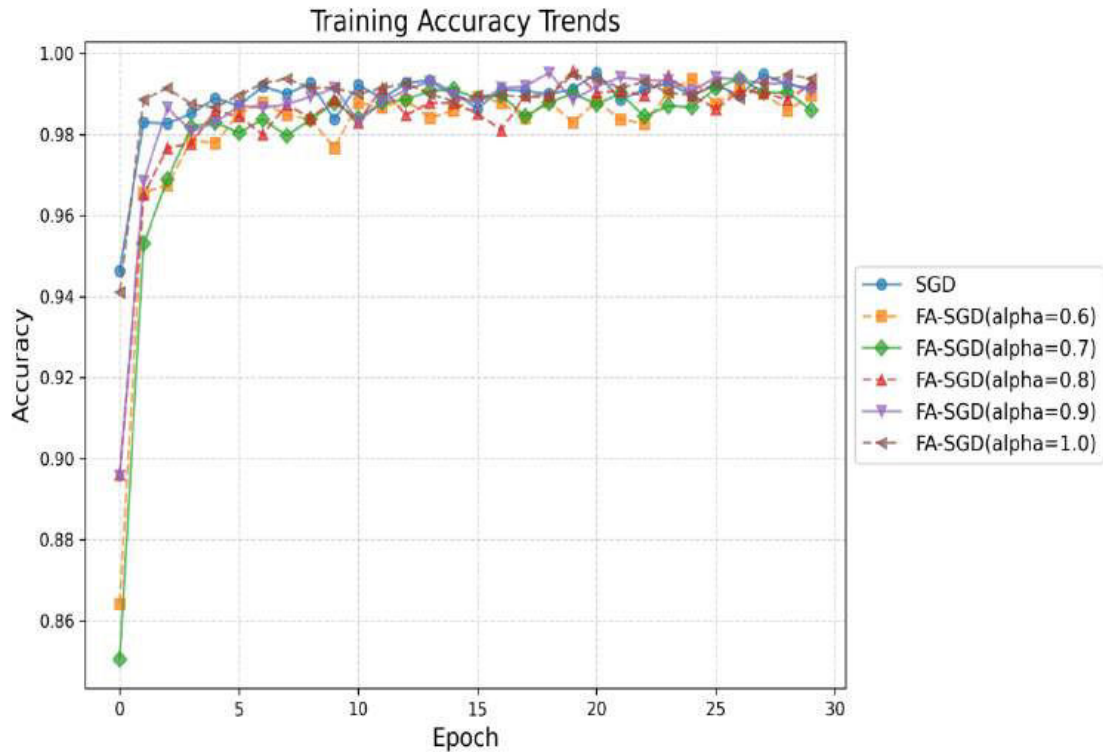


**Fig-32: Combined Learning Curve visualization of training accuracy trends for Study-II**

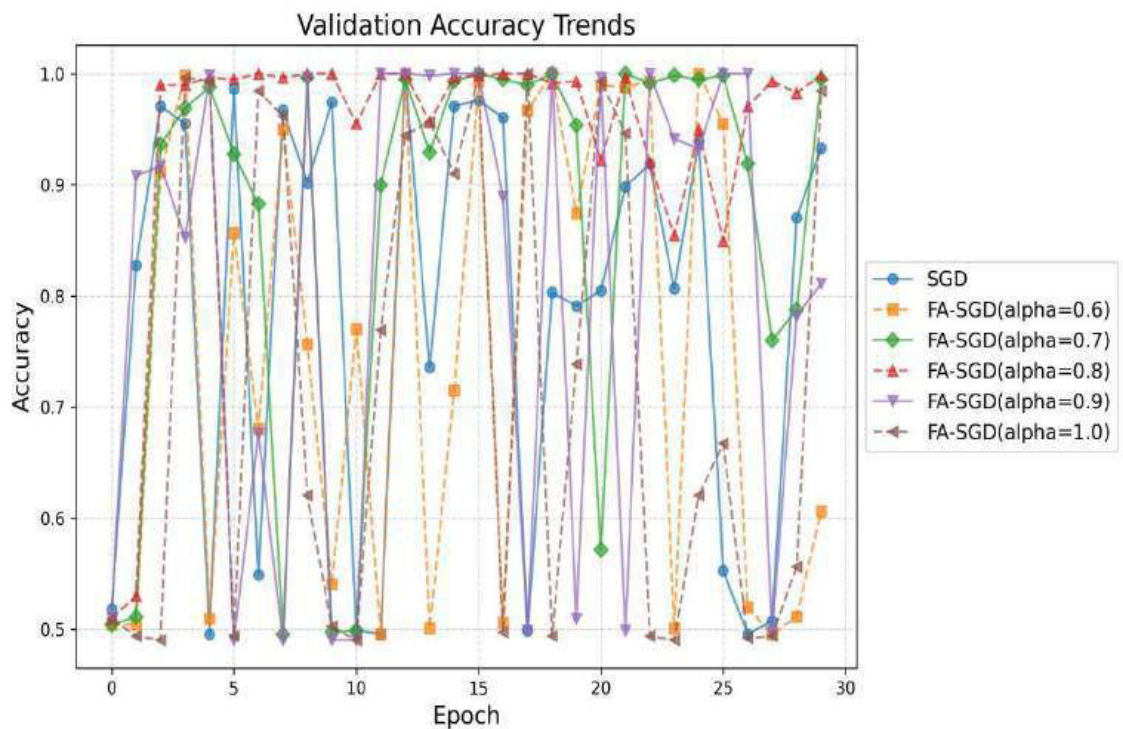


**Fig-33: Combined Learning Curve visualization of validation accuracy trends for Study-II**

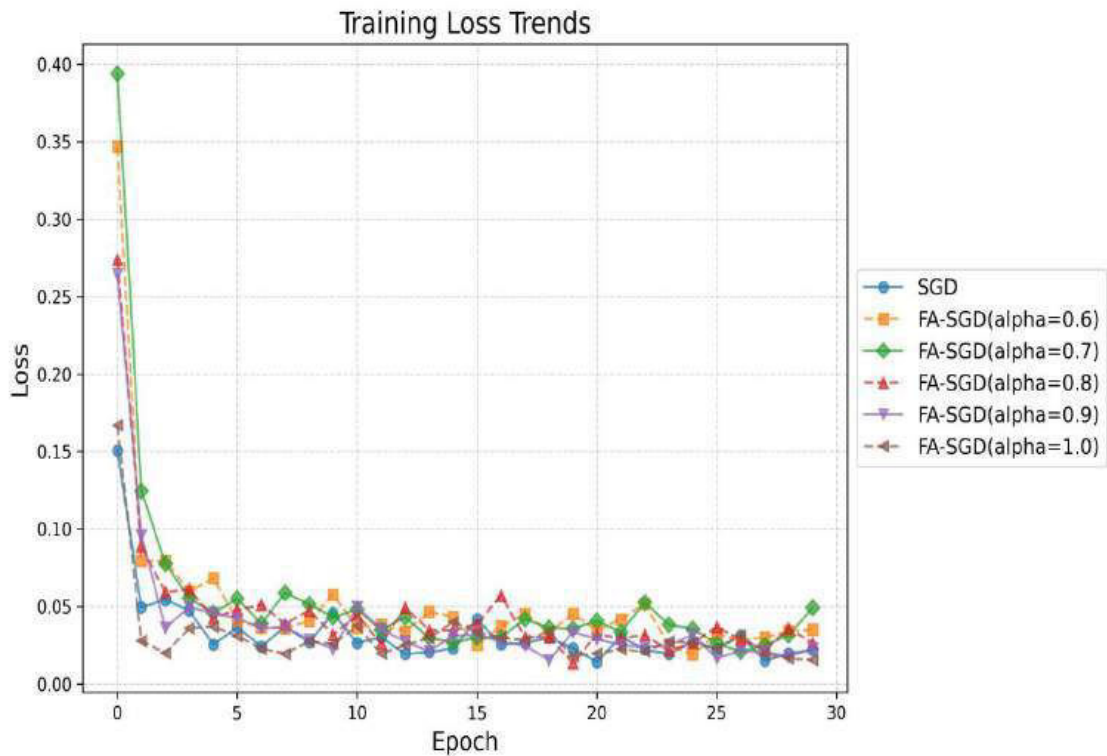


**Fig-34: Combined Learning Curve visualization of training loss trends for Study-II**

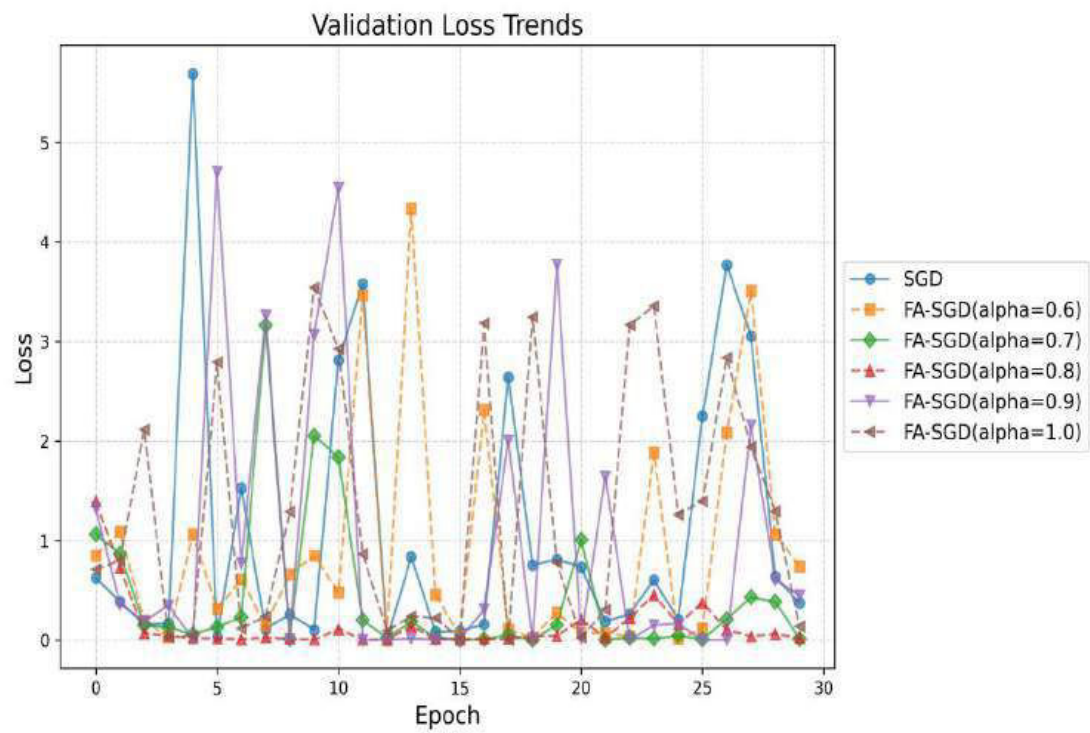


**Fig-35: Combined Learning Curve visualization of validation loss trends for Study-II**

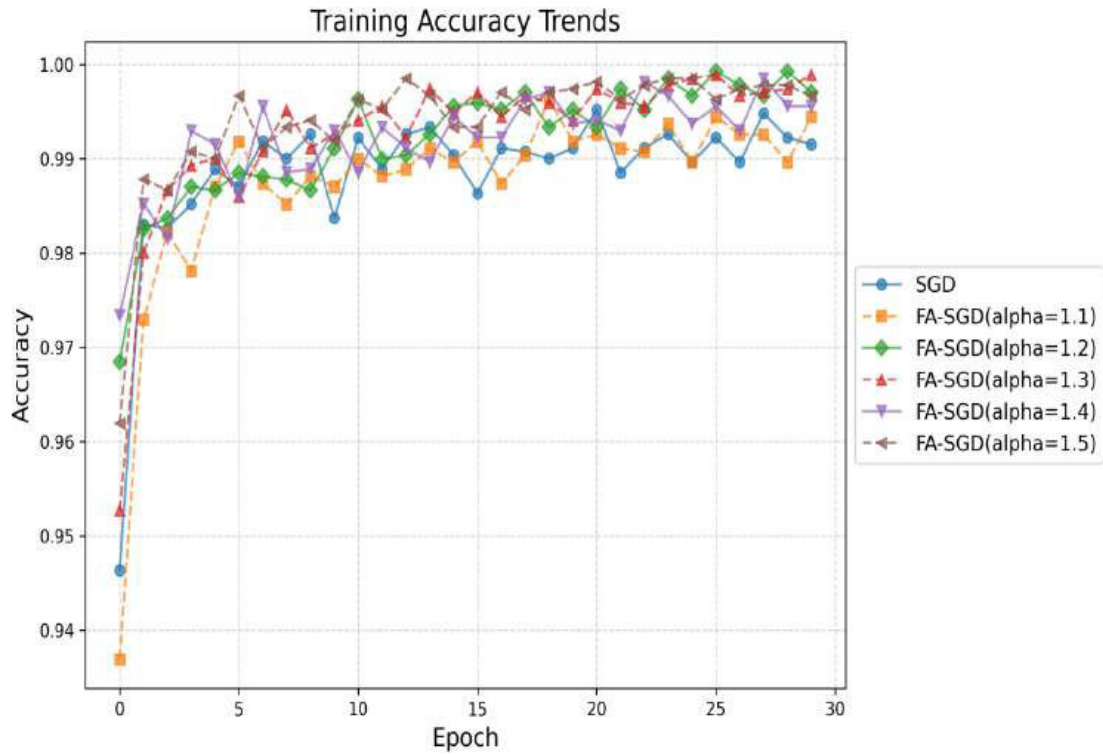


**Fig-36: Combined Learning Curve visualization of training accuracy trends for Study-III**

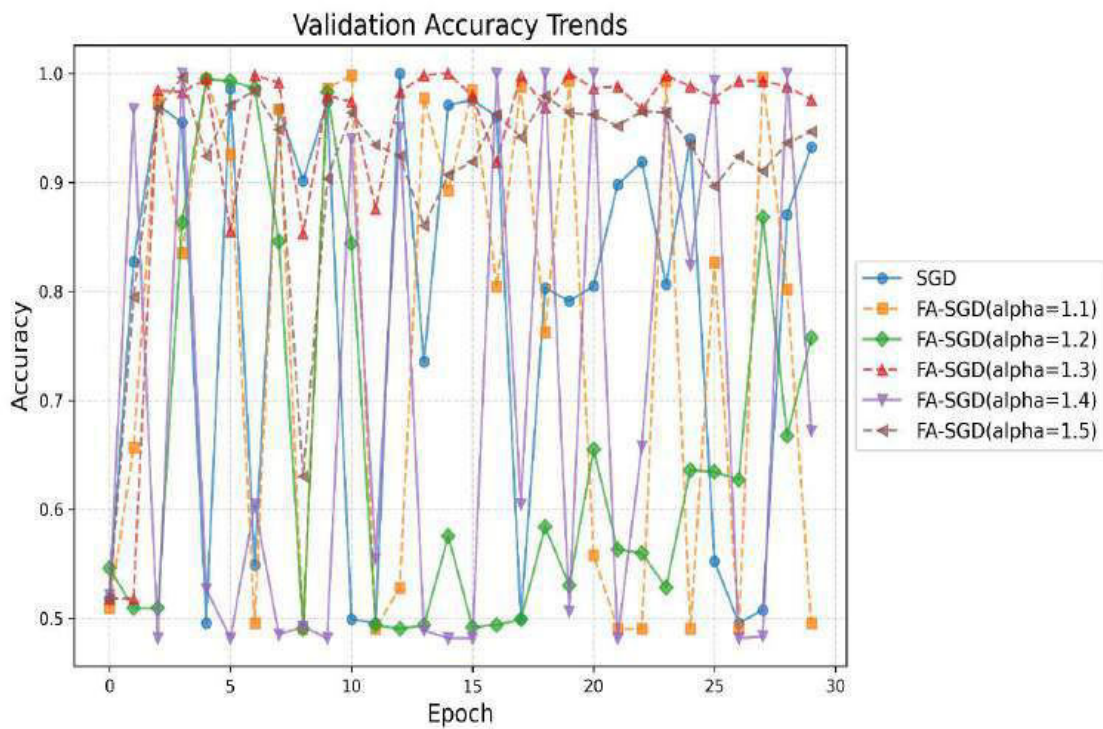


**Fig-37: Combined Learning Curve visualization of validation accuracy trends for Study-III**

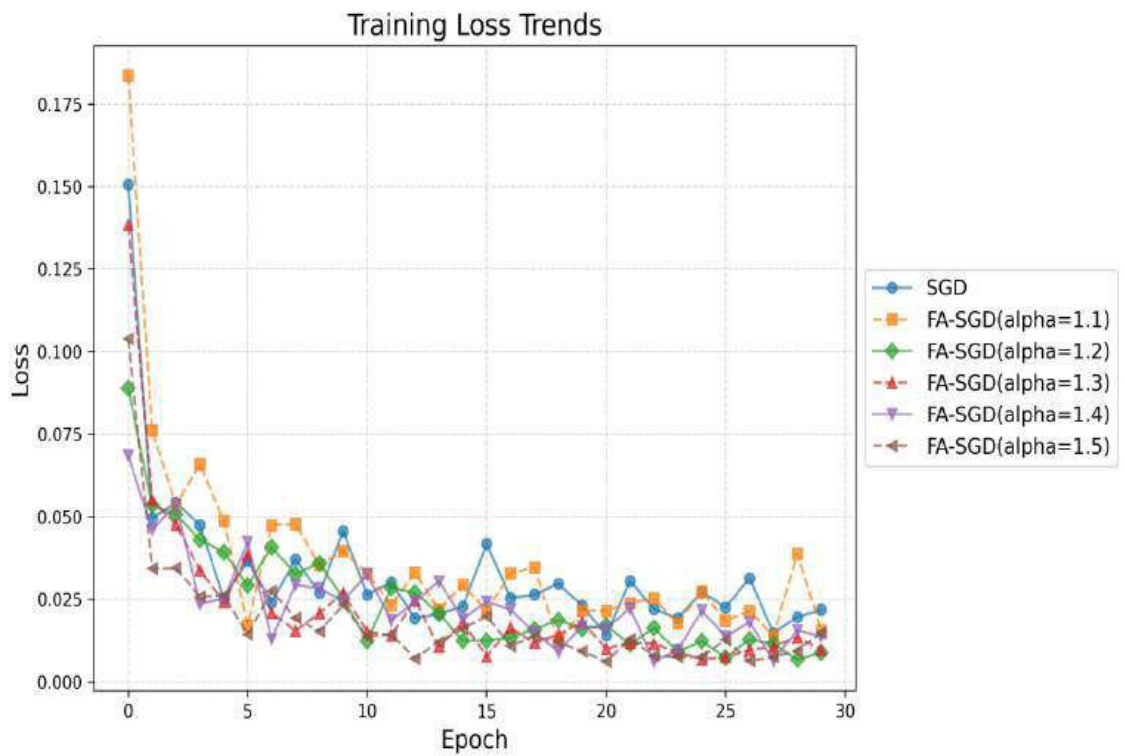


**Fig-38: Combined Learning Curve visualization of training loss trends for Study-III**

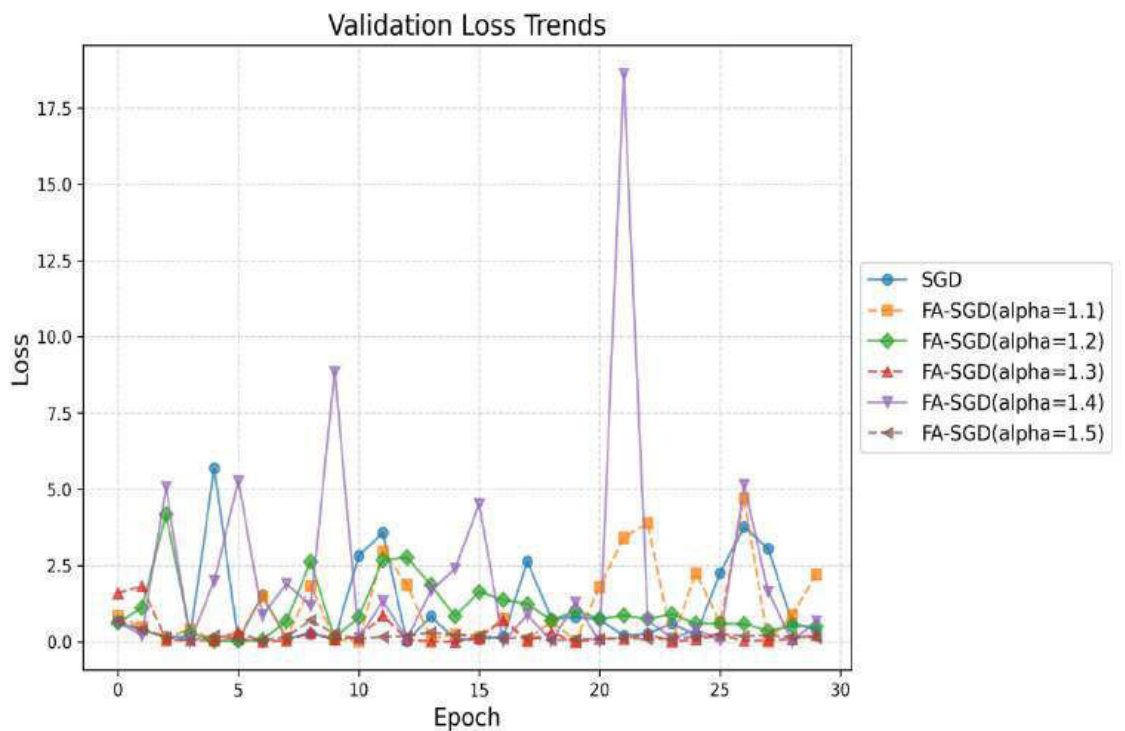


**Fig-39: Combined Learning Curve visualization of validation loss trends for Study-III**



**Fig-40: Combined Learning Curve visualization of training accuracy trends for Study-IV**

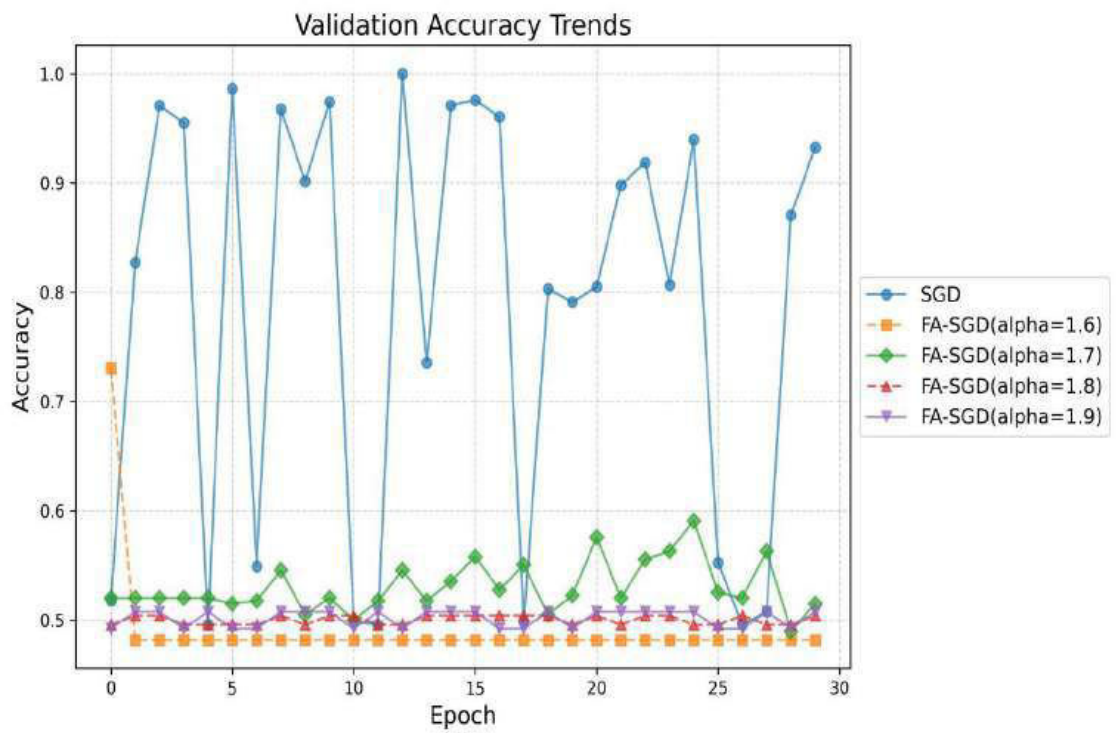


**Fig-41: Combined Learning Curve visualization of validation accuracy trends for Study-IV**

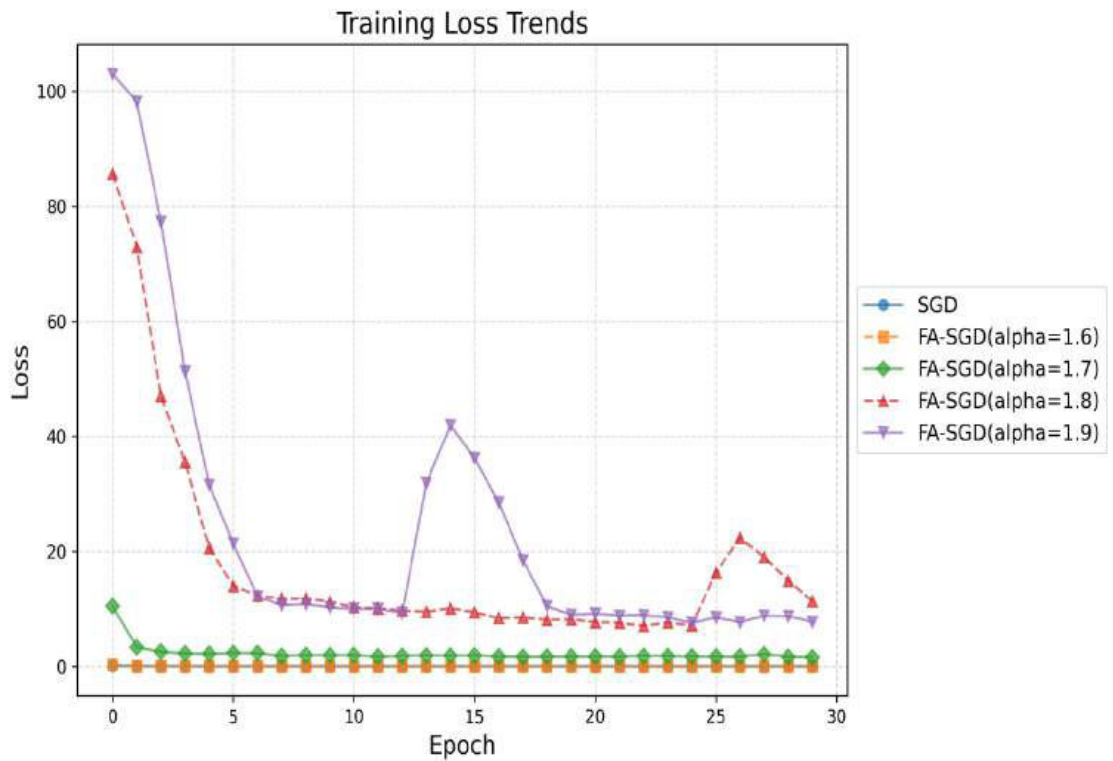


**Fig-42: Combined Learning Curve visualization of training loss trends for Study-IV**

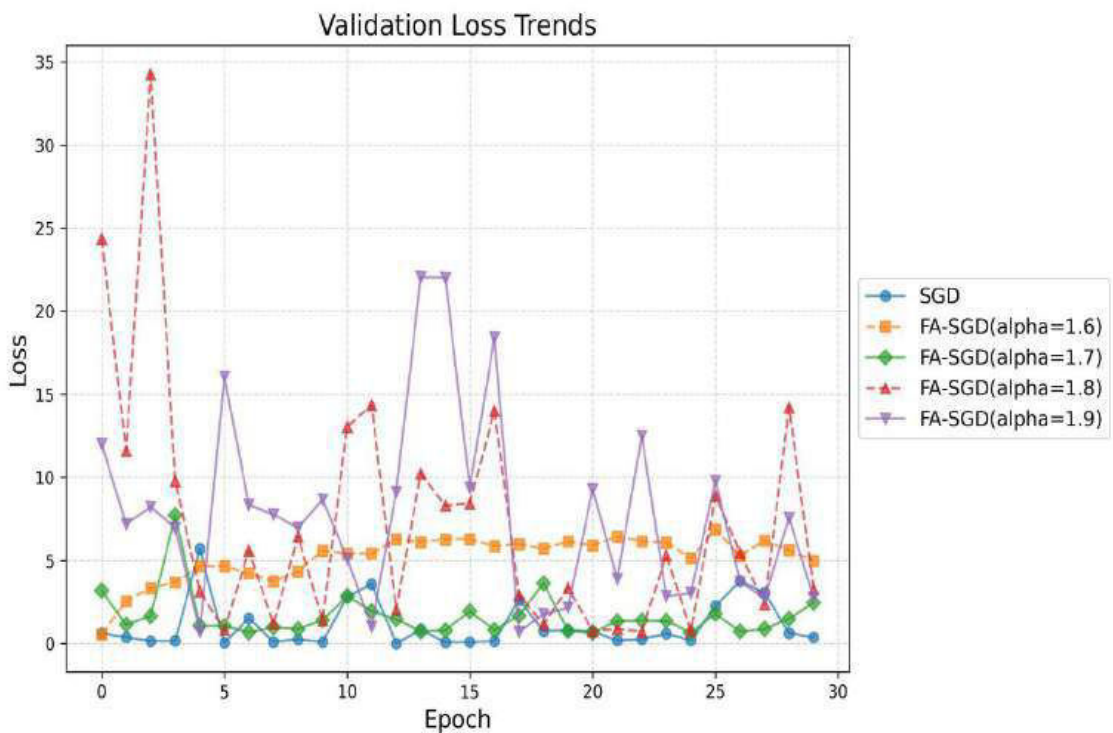


**Fig-43: Combined Learning Curve visualization of validation loss trends for Study-IV**



**Fig-44: Interpretable Predictions by Ultralight CNN Architecture**

#### 4.9 Summary

This chapter contains the simulations of the proposed strategy for signature classification on benchmark CEDAR dataset, after the selection of tuned hyperparameters, which are consistently applied to the proposed model throughout entire study. Also includes the performance analysis of suggested model with the standard SGD and the novel FA-SGD in terms of Precision, Recall, Accuracy, and F1-Score. The next chapter reviews the results obtained in Chapter 4 in relation to original problem.

## CHAPTER 5

# CONCLUSIONS AND FUTURE WORK

### 5.1 Introduction

This chapter outlines conclusions deduced from suggested CNN model along with FA-SGD optimization strategy for signature verification task, discussed in the previous chapters. Apart from conclusions, it also provides guidelines to scholars for future endeavours. They can apply proposed method or variations in it for various image classification tasks.

### 5.2 Conclusions

The main aim of conducted research is to analyze and accentuate the abilities of fractional calculus based FA-SGD optimization algorithm and the ultralight CNN model for authentication of handwritten signatures. The conclusions deduced from research are as follows.

- The combination of ultralight CNN model and fractionally accelerated SGD optimizer has demonstrated notable performance in signature verification task.
- Ultralight CNN model has resulted in significant decrease in computational resources due to its simple architecture as opposed to complex architectures mentioned in the literature, making it a suitable option to be deployed in resource-limited devices.
- The robust capabilities of fractional calculus and DL is highlighted for achieving accurate and efficient classification of signatures.
- It is depicted that the suggested CNN model with FA-SGD optimizer, learning rate of 0.001, alpha value of 0.7 and with the batch size of 128 has outperformed the present SOTA models on benchmark CEDAR database.

- This study offers robust, reliable, efficient, resource friendly and accurate model for classification of handwritten signatures.

### 5.3 Future Work

- The vital research direction is to merge FA-SGD optimizer with various other deep learning models for image classification tasks.
- The proposed ultralight CNN model can be redesigned to further reduce computational complexity by reducing no of filters, employing smaller Kernel size, employing mobile inverted bottleneck blocks to reduce dynamic separable convolutions with out compromising on feature extraction, employing knowledge distillation technique, and by employing model quantization and weight sharing.
- The proposed FA-SGD optimization strategy can be redesigned using Fractional Calculus-based concepts (fractional-order gradients), as it employs fractional order derivatives; thus, it can potentially provide faster convergence and more accurate imageclassification.

## References

- [1] Harakannanavar, S.S., P.C. Renukamurthy, and K.B. Raja, Comprehensive study of biometric authentication systems, challenges and future trends. *International Journal of Advanced Networking and Applications*, 2019. 10(4): p. 3958-3968.
- [2] Beltrán, M. and M. Calvo, A privacy threat model for identity verification based on facial recognition. *Computers & Security*, 2023. 132: p. 103324.
- [3] Garg, V., A. Singhal, and P. Tiwari. A study on transformation in technological based biometrics attendance system: human resource management practice. in 2018 8th International Conference on Cloud Computing, Data Science & Engineering (Confluence). 2018. IEEE.
- [4] Awad, A.I. and A.E. Hassanien, Impact of some biometric modalities on forensic science. *Computational intelligence in digital forensics: Forensic investigation and applications*, 2014: p. 47-62.
- [5]. Mason, J., et al., An investigation of biometric authentication in the healthcare environment. *Array*, 2020. 8: p. 100042.
- [6] Mróz-Gorgoń, B., et al., Biometrics innovation and payment sector perception. *Sustainability*, 2022. 14(15): p. 9424.
- [7] Dubey, A., Z. Saquib, and S. Dwivedi. Electronic authentication for e-Government services—A survey. in 10th IET System Safety and Cyber-Security Conference 2015. 2015. IET.
- [8] Hernandez-de-Menendez, M., et al., Biometric applications in education. *International Journal on Interactive Design and Manufacturing (IJIDeM)*, 2021. 15: p. 365-380.
- [9] Rodgers, W., et al., Artificial intelligence-driven music biometrics influencing customers' retail buying behavior. *Journal of Business Research*, 2021. 126: p. 401-414.
- [10] Nanni, L., S. Ghidoni, and S. Brahnam, Handcrafted vs. non-handcrafted features for computer vision classification. *Pattern recognition*, 2017. 71: p. 158-172.

[11] Hafemann, L.G., R. Sabourin, and L.S. Oliveira. Offline handwritten signature verification—Literature review. in 2017 seventh international conference on image processing theory, tools and applications (IPTA). 2017. IEEE.

[12] Kaur, H. and M. Kumar, Signature identification and verification techniques: state-of-the-art work. *Journal of Ambient Intelligence and Humanized Computing*, 2023. 14(2): p. 1027-1045.

[13] Li, Z., et al., A survey of convolutional neural networks: analysis, applications, and prospects. *IEEE transactions on neural networks and learning systems*, 2021. 33(12): p. 6999-7019.

[14] Yapici, M.M., A. Tekerek, and N. Topaloglu. Convolutional neural network based offline signature verification application. in 2018 International Congress on Big Data, Deep Learning and Fighting Cyber Terrorism (IBIGDELFT). 2018. IEEE.

[15] Das, S., et al., Recurrent neural networks (RNNs): architectures, training tricks, and introduction to influential research. *Machine Learning for Brain Disorders*, 2023: p. 117-138.

[16] Ghosh, R., A Recurrent Neural Network based deep learning model for offline signature verification and recognition system. *Expert Systems with Applications*, 2021. 168: p. 114249.

[17] Islam, M.T., et al. Image recognition with deep learning. in 2018 International conference on intelligent informatics and biomedical sciences (ICIIBMS). 2018. IEEE.

[18] Thakare, B.S. and H.R. Deshmukh. A combined feature extraction model using SIFT and LBP for offline signature verification system. in 2018 3rd International Conference for Convergence in Technology (I2CT). 2018. IEEE.

[19] Guest, R. and O. Miguel-Hurtado. Enhancing static biometric signature verification using Speeded-Up Robust Features. in 2012 IEEE International Carnahan Conference on Security Technology (ICCST). 2012. IEEE.

- [20] Nguyen, V., M. Blumenstein, and G. Leedham. Global features for the off-line signature verification problem. in 2009 10th International Conference on Document Analysis and Recognition. 2009. IEEE.
- [21] Miguel-Hurtado, O., et al. On-line signature verification by dynamic time warping and gaussian mixture models. in 2007 41st annual IEEE international Carnahan conference on security technology. 2007. IEEE.
- [22] Hadjadj, B., Y. Chibani, and H. Nemmour, An efficient open system for offline handwritten signature identification based on curvelet transform and one-class principal component analysis. Neurocomputing, 2017. 265: p. 66-77.
- [23] Pourshahabi, M.R., M.H. Sigari, and H.R. Pourreza. Offline handwritten signature identification and verification using contourlet transform. in 2009 International Conference of Soft Computing and Pattern Recognition. 2009. IEEE.
- [24] Ling, X., et al. On-line signature verification based on Gabor features. in The 19th Annual Wireless and Optical Communications Conference (WOCC 2010). 2010. IEEE.
- [25] Tolosana, R., et al., DeepSign: Deep on-line signature verification. IEEE Transactions on Biometrics, Behavior, and Identity Science, 2021. 3(2): p. 229-239.
- [26] Szegedy, C., et al. Going deeper with convolutions. in Proceedings of the IEEE conference on computer vision and pattern recognition. 2015.
- [27] Alzubaidi, L., et al., Review of deep learning: concepts, CNN architectures, challenges, applications, future directions. Journal of big Data, 2021. 8: p. 1-74.
- [28] Szegedy, C., et al. Inception-v4, inception-resnet and the impact of residual connections on learning. in Proceedings of the AAAI conference on artificial intelligence. 2017.
- [29] He, K., et al. Deep residual learning for image recognition. in Proceedings of the IEEE conference on computer vision and pattern recognition. 2016.

[30] Krizhevsky, A., I. Sutskever, and G.E. Hinton, Imagenet classification with deep convolutional neural networks. *Advances in neural information processing systems*, 2012. 25.

[31] Xie, S., et al. Aggregated residual transformations for deep neural networks. in *Proceedings of the IEEE conference on computer vision and pattern recognition*. 2017.

[32] Khan, Z.A., N.I. Chaudhary, and S. Zubair, Fractional stochastic gradient descent for recommender systems. *Electronic Markets*, 2019. 29: p. 275-285.

[33] Khan, Z.A., et al., Design of normalized fractional SGD computing paradigm for recommender systems. *Neural Computing and Applications*, 2020. 32: p. 10245-10262.

[34] Khan, Z.A., et al., Design of momentum fractional stochastic gradient descent for recommender systems. *IEEE Access*, 2019. 7: p. 179575-179590.

[35] Wei, Y., et al., Generalization of the gradient method with fractional order gradient direction. *Journal of the Franklin Institute*, 2020. 357(4): p. 2514-2532.

[36] Khan, Z.A., N.I. Chaudhary, and M.A.Z. Raja, Generalized fractional strategy for recommender systems with chaotic ratings behavior. *Chaos, Solitons & Fractals*, 2022. 160: p. 112204.

[37] Stauffer, M., et al. Offline signature verification using structural dynamic time warping. in *2019 International Conference on Document Analysis and Recognition (ICDAR)*. 2019. IEEE.

[38] Sharif, M., et al., A framework for offline signature verification system: Best features selection approach. *Pattern Recognition Letters*, 2020. 139: p. 50-59.

[39] Gopika, S., Online and offline signature verification: a combined approach. *Procedia Computer Science*, 2015. 46: p. 1593-1600.

[40] Chandra, S. and S. Maheskar. Offline signature verification based on geometric feature extraction using artificial neural network. in *2016 3rd international conference on recent advances in information technology (RAIT)*. 2016. IEEE.

[41] Azmi, A.N., D. Nasien, and F.S. Omar, Biometric signature verification system based on freeman chain code and k-nearest neighbor. *Multimedia Tools and Applications*, 2017. 76: p. 15341-15355.

[42] Sharma, N., et al., Siamese convolutional neural network-based twin structure model for independent offline signature verification. *Sustainability*, 2022. 14(18): p. 11484.

[43] Shariatmadari, S., S. Emadi, and Y. Akbari, Patch-based offline signature verification using one-class hierarchical deep learning. *International Journal on Document Analysis and Recognition (IJDAR)*, 2019. 22(4): p. 375-385.

[44] Wei, P., H. Li, and P. Hu. Inverse discriminative networks for handwritten signature verification. in *Proceedings of the IEEE/CVF Conference on Computer Vision and Pattern Recognition*. 2019.

[45] Roy, S., et al., Offline signature verification system: a graph neural network based approach. *Journal of Ambient Intelligence and Humanized Computing*, 2023: p. 1-11.

[46] Parcham, E., M. Ilbeygi, and M. Amini, CBCapsNet: A novel writer-independent offline signature verification model using a CNN-based architecture and capsule neural networks. *Expert Systems with Applications*, 2021. 185: p. 115649.

[47] Chattopadhyay, S., et al. SURDS: Self-supervised attention-guided reconstruction and dual triplet loss for writer independent offline signature verification. in *2022 26th International Conference on Pattern Recognition (ICPR)*. 2022. IEEE.

[48] Sanmorino, A. and S. Yazid. A survey for handwritten signature verification. in *2012 2nd International Conference on Uncertainty Reasoning and Knowledge Engineering*. 2012. IEEE.

[49] Alsuhimat, F.M. and F.S. Mohamad, A Hybrid Method of Feature Extraction for Signatures Verification Using CNN and HOG a Multi-Classification Approach. *IEEE Access*, 2023. 11: p. 21873-21882.

[50] Park, C.-Y., H.-G. Kim, and H.-J. Choi. Robust online signature verification using long-term recurrent convolutional network. in 2019 IEEE International Conference on Consumer Electronics (ICCE). 2019. IEEE.

[51] Eskander, G.S., R. Sabourin, and E. Granger. Adaptation of writer-independent systems for offline signature verification. in 2012 International Conference on Frontiers in Handwriting Recognition. 2012. IEEE.

[52] Eskander, G.S., R. Sabourin, and E. Granger, Hybrid writer-independent–writer-dependent offline signature verification system. *IET biometrics*, 2013. 2(4): p. 169-181.

[53] Kao, H.-H. and C.-Y. Wen, An offline signature verification and forgery detection method based on a single known sample and an explainable deep learning approach. *Applied Sciences*, 2020. 10(11): p. 3716.

[54] Hirunyawanakul, A., et al., Deep learning technique for improving the recognition of handwritten signature. *Int. J. Inform. Electron. Eng*, 2019. 9(4): p. 72-78.

[55] Mitchell, A., et al., Off line signature verification using transfer learning and data Augmentation on Imbalanced Dataset.

[56] Mersa, O., et al. Learning representations from persian handwriting for offline signature verification, a deep transfer learning approach. in 2019 4th International conference on pattern recognition and image analysis (IPRIA). 2019. IEEE.

[57] Jampour, M., S. Abbaasi, and M. Javidi, CapsNet regularization and its conjugation with ResNet for signature identification. *Pattern Recognition*, 2021. 120: p. 107851.

[58] Sam, S.M., et al., Offline signature verification using deep learning convolutional neural network (CNN) architectures GoogLeNet inception-v1 and inception-v3. *Procedia Computer Science*, 2019. 161: p. 475-483.

[59] Gumusbas, D. and T. Yildirim. Offline signature identification and verification using capsule network. in 2019 IEEE international symposium on innovations in intelligent systems and applications (INISTA). 2019. IEEE.

[60] Muhtar, Y., et al., Fc-resnet: A multilingual handwritten signature verification model using an improved resnet with cbam. *Applied Sciences*, 2023. 13(14): p. 8022.

[61] Tanko, O., et al. A Writer-Dependent Approach for Offline Signature Verification Using Feature Learning and One-Class Support Vector Machine. in 2023 3rd International Conference on Electrical, Computer, Communications and Mechatronics Engineering (ICECCMEE). 2023. IEEE.

[62] Bagherinezhad, H., M. Rastegari, and A. Farhadi. Lcnn: Lookup-based convolutional neural network. in Proceedings of the IEEE conference on computer vision and pattern recognition. 2017.

[63] Rastegari, M., et al. Xnor-net: Imagenet classification using binary convolutional neural networks. in European conference on computer vision. 2016. Springer.

[64] Zou, J., et al., Convolutional neural network simplification via feature map pruning. *Computers & Electrical Engineering*, 2018. 70: p. 950-958.

[65] He, Y., X. Zhang, and J. Sun. Channel pruning for accelerating very deep neural networks. in Proceedings of the IEEE international conference on computer vision. 2017.

[66] Parashar, A., et al., Data preprocessing and feature selection techniques in gait recognition: A comparative study of machine learning and deep learning approaches. *Pattern Recognition Letters*, 2023. 172: p. 65-73.

[67] Love, P.E., et al., Explainable artificial intelligence (XAI): Precepts, models, and opportunities for research in construction. *Advanced Engineering Informatics*, 2023. 57: p. 102024.

[68] Ribeiro, M.T., S. Singh, and C. Guestrin. " Why should i trust you?" Explaining the predictions of any classifier. in Proceedings of the 22nd ACM SIGKDD international conference on knowledge discovery and data mining. 2016.

[69] Adadi, A. and M. Berrada, Peeking inside the black-box: a survey on explainable artificial intelligence (XAI). *IEEE access*, 2018. 6: p. 52138-52160.

[70] Palatnik de Sousa, I., M. Maria Bernardes Rebuzzi Vellasco, and E. Costa da Silva, Local interpretable model-agnostic explanations for classification of lymph node metastases. *Sensors*, 2019. 19(13): p. 2969.

[71] Alber, M., et al., iNNvestigate neural networks! *Journal of machine learning research*, 2019. 20(93): p. 1-8.

[72] Holzinger, A., et al. Explainable AI methods-a brief overview. in *International workshop on extending explainable AI beyond deep models and classifiers*. 2022. Springer.

[73] Xue, H., Fractional-order gradient descent with momentum for RBF neural network-based AIS trajectory restoration. *Soft Computing*, 2021. 25(2): p. 869-882.

[74] Xie, J. and S. Li, Training Neural Networks by Time-Fractional Gradient Descent. *Axioms*, 2022. 11(10): p. 507.